UNIVERSITÉ DE MONTRÉAL

MODELING OF THE THERMOMECHANICAL BEHAVIOR OF AN EPOXY RESIN
SUBJECTED TO ELEVATED TEMPERATURES AND EXPERIMENTAL
VERIFICATION

FRANÇOIS LANDRY
DÉPARTEMENT DE GÉNIE MÉCANIQUE
ÉCOLE POLYTECHNIQUE DE MONTRÉAL

MÉMOIRE PRÉSENTÉ EN VUE DE L'OBTENTION DU DIPLÔME DE
MAÎTRISE ÈS SCIENCES APPLIQUÉES
(GÉNIE MÉCANIQUE)
AOÛT 2010

UNIVERSITÉ DE MONTRÉAL

ÉCOLE POLYTECHNIQUE DE MONTRÉAL

Ce mémoire intitulé :

MODELING OF THE THERMOMECHANICAL BEHAVIOR OF AN EPOXY RESIN
SUBJECTED TO ELEVATED TEMPERATURES AND EXPERIMENTAL
VERIFICATION

présenté par : LANDRY, François

en vue de l'obtention du diplôme de : Maîtrise ès Sciences Appliquées

a été dûment accepté par le jury d'examen constitué de :

Mme. VILLEMURE, Isabelle, Ph.D., présidente

M. LÉVESQUE, Martin, Ph.D., membre et directeur de recherche

Mme. LI, Chun, Ph.D., membre et codirectrice de recherche

Mme. MULIANA, Anastasia Hanifah, Ph.D., membre

À mes parents

ACKNOWLEDGMENT

RÉSUMÉ

Ce travail présente une étude sur le comportement thermomécanique d'une résine époxy. Un montage expérimental a d'abord été développé afin de pouvoir réaliser des essais mécaniques sur des matériaux polymères à haute température. Ce montage permettait d'appliquer sur les échantillons des histoires de chargement complexes en contrainte et température, tout en permettant une mesure précise de la charge appliquée, de la déformation induite, de la température et du déplacement des mâchoires hydrauliques. Le montage fut utilisé afin d'étudier la réponse de la résine époxy à la fois selon des tests isothermes de fluage-recouvrance uniaxial ainsi que selon des histoires de chargement complexes en contrainte et température.

Le comportement de la résine fut caractérisé d'après un nouveau modèle viscoélastique non linéaire de type Schapery. L'étude a d'abord tenté de vérifier la pertinence d'utiliser des données provenant de tests de fluage-recouvrance réalisés dans des conditions isothermes afin de déterminer les paramètres du modèle et prédire la réponse du matériau dans des conditions thermomécaniques complexes. Puis, des données provenant à la fois des courbes de fluage-recouvrance isothermes et des histoires de chargement complexes en contrainte et température furent utilisées afin d'obtenir les paramètres du modèle. Les résultats démontrèrent que cette approche ne permettait pas d'obtenir une amélioration significative des prédictions du modèle. Les paramètres du modèle de comportement furent finalement obtenus selon une nouvelle approche utilisant seulement l'information fournie par les histoires de chargement complexes en contrainte et température. Le modèle obtenu fut vérifié en comparant les données expérimentales avec les prédictions du modèle pour des essais de fluage-recouvrance. Les prédictions du modèle identifié avec cet ensemble de données ont fourni des résultats satisfaisants. Ces résultats présentent une source de motivation pour de futures recherches visant à concevoir des tests optimisés afin d'obtenir des paramètres fiables avec un nombre limité de données expérimentales.

ABSTRACT

This work presents a study of the thermo-mechanical behavior of an epoxy resin. An experimental setup was initially developed to perform mechanical tests on polymers at high temperature. The setup allowed applying complex stress and temperature histories while delivering precise load, strain, temperature and displacement measurement. The setup was used to investigate the response of the epoxy resin through both unixial isothermal creep-recovery tests as well as time varying stress and temperature histories.

The material response was predicted using a new Schapery-type constitutive model. Characterization of the epoxy resin was firstly done using isothermal creep and recovery data at different temperatures and stress levels. The accuracy of this standard modeling approach was then validated under complex loading and temperature histories. Next, data coming from transient stress and temperature load histories were used together with isothermal creep and recovery curves to obtain the material parameters. Results shown that the approach did not significantly help obtaining a better representation of the material behavior. The parameters of the constitutive model were also obtained according to a new approach that consists of using the limited amount of data provided by one complex stress and temperature history. The model obtained was verified by comparing experimental data and predicted responses of various isothermal creep and recovery curves. Results were acceptable and represent a motivation for future research aiming at designing optimized tests to obtain reliable viscoelastic models using a limited amount of experimental data.

CONDENSÉ EN FRANÇAIS

1. Introduction

L'utilisation des Matériaux Composites à Matrice Polymère (MCMP) dans l'industrie aérospatiale pour le remplacement de composantes métalliques a continué de progresser durant la dernière décennie. Le principal avantage de ce remplacement touche la réduction du poids des composantes, conduisant ainsi à des économies de carburant.

Certaines composantes à proximité des moteurs doivent cependant soutenir des températures en service très élevées. Dans de telles conditions, les MCMP sont susceptibles de présenter un comportement viscoélastique. De plus, la température peut accélérer le processus de vieillissement de la matrice polymère. Une modélisation réaliste du comportement de ce type de matériau doit considérer ces effets et utiliser des données expérimentales représentatives du comportement thermomécanique du matériau.

Cette étude fait partie d'un programme de recherche collaboratif visant à développer de nouvelles méthodologies pour prédire le comportement mécanique des MCMP à haute température. Le travail vise essentiellement deux objectifs, soit le développement d'un dispositif expérimental permettant de réaliser des essais mécaniques sur des matériaux polymères à haute température et l'élaboration d'une loi de comportement dépendante de la contrainte et de la température pour une résine époxy.

2. Comportement des matériaux polymères

Les polymères présentent un comportement viscoelastique influencé par l'histoire de chargement. Les réponses en contrainte et en déformation des matériaux viscoelastiques dépendent

ainsi du temps et de la vitesse d'application du chargement. Par exemple, deux essais de traction réalisés à deux différentes vitesses de déformation peuvent conduire à des réponses en contrainte considérablement distinctes.

Le comportement d'un matériau viscoélastique est traditionnellement caractérisé par la nature de sa réponse à deux types de tests mécaniques : des essais de fluage-recouvrance et des essais de relaxation. Ces tests mécaniques permettent de définir les propriétés propres aux matériaux telles le module d'élasticité et la souplesse. La réalisation d'essais mécaniques à température élevée conduit cependant à certaines difficultés techniques. La mesure de la déformation induite et le contrôle de la température sont notamment deux éléments importants à considérer afin d'assurer la fiabilité et la précision des résultats expérimentaux.

3. Techniques de modélisation des matériaux viscoélastiques

L'effet de la température sur les matériaux polymères a été largement étudié dans la littérature et divers modèles viscoélastiques permettent de caractériser leur comportement, notamment des modèles linéaires, l'utilisation du Principe de Superposition Temps-Temperature (PSTT) et le modèle non linéaire de Schapery.

La plupart des matériaux polymères manifestent une réponse viscoelastique linéaire pour certaines plages de contraintes et de températures. L'utilisation d'un modèle linéaire peut, cependant, ne pas caractériser adéquatement l'ensemble du comportement thermomécanique des polymères. Pour des niveaux de contrainte et de température excédant les limites du modèle linéaire, l'utilisation de modèles viscoélastiques non linéaires peut conduire à des résultats plus précis.

L'effet de la température sur le comportement viscoélastique des polymères a été largement étudié avec le PSTT. Ce principe permet de comparer entre elles les réponses des essais de

fluage et de relaxation obtenues à des températures différentes. Le concept implique que les temps de relaxation, qui augmentent avec la température, peuvent être liés à ceux d'une température de référence par un simple facteur multiplicatif. Les matériaux qui peuvent être complètement caractérisés par le biais du PSTT sont classés comme étant des matériaux thermorhéologiquement simple (MTS), tandis que les matériaux qui ne respectent pas le PSTT sont appelés matériaux thermorhéologiquement complexes (MTC).

Les MTC manifestent un comportement nécessitant des modèles viscoélastiques plus complexes, comme le modèle non linéaire de Schapery. Dans ce modèle, les propriétés du matériau sont définies en utilisant des paramètres viscoélastiques linéaires et des fonctions non-linéarisantes. Ces fonctions sont utilisées pour introduire les non linéarités induites par les contraintes, la température, l'humidité, le vieillissement, etc.

Par ailleurs, les paramètres de ces modèles viscoélastiques sont communément obtenus en utilisant des histoires de contraintes et de températures qui ne sont pas forcément représentatives du comportement général du matériau à caractériser. Les modèles utilisent généralement des données provenant d'essais de fluage-recouvrance réalisés dans des conditions isothermes.

4. Définition des objectifs du travail

Cette étude consistait à étudier la réponse thermomécanique d'une résine polymère sous diverses histoires de chargement en contrainte et en température. Le travail comportait deux principaux objectifs, étant :

1. Développer un montage expérimental permettant de réaliser des essais mécaniques fiables et précis à haute température sur des matériaux polymères.

2. Vérifier l'efficacité de l'approche conventionnelle consistant à utiliser des essais de fluage-recouvrance en condition isotherme afin de déterminer les propriétés viscoélas-

tiques non linéaires d'une résine polymère et prédire la réponse en déformation du matériau sous des histoires complexes en contrainte et en température.

5. Développement du montage et des essais expérimentaux

La première étape du projet consistait donc au développement du montage expérimental. Afin de respecter les exigences définies par le projet et de permettre l'obtention de données fiables et précises, le montage fut développé en considérant les normes ASTM reliées aux essais à effectuer.

Le montage expérimental reposait sur une machine d'essai universelle MTS 810 et était composé d'un four à haute température MTS 653.04 possédant trois zones chauffées, indépendamment contrôlées par un contrôleur de température MTS 409.83 . La machine d'essai MTS possédait une cellule de charge de 25 kN ainsi que des mors hydrauliques refroidis à l'eau. Pour les essais de fluage-recouvrance, les déformations furent mesurées en utilisant un extensomètre haute température MTS 632.42. Des jauges de déformations Vishay EA-06-125TM furent par contre préférées à l'extensomètre durant les essais de traction à vitesse de déplacement constante afin d'éviter d'endommager l'appareil en cas de rupture des éprouvettes.

La température de l'échantillon était contrôlée en ajustant la température de l'air à l'intérieur du four avec le contrôleur MTS afin d'obtenir une température uniforme de l'échantillon. Un appareil fut spécialement conçu afin de pouvoir facilement positionner trois thermocouples dans la zone test de l'échantillon et pouvoir lire la température directement sur la surface du matériau. Le dispositif permit d'améliorer le contrôle de la température et d'obtenir une meilleure fiabilité des mesures.

Le matériau étudié consistait en une résine époxy EPON 862 mélangé avec un agent de durcisseur EPIKURE 3300 à 24.8phr. Le système époxy subit une cuisson de 10 heures à

température ambiante, 1.5 heures à 82°C et 1.5 heures à 150°C. Les éprouvettes de traction furent découpées au jet d'eau à partir des panneaux de résine obtenus. Des éprouvettes ASTM type I furent utilisés pour tous les tests réalisés.

Des essais de traction à vitesse constante ont été menés sur la résine époxy à différentes températures fixes, variant de 25°C à 90°C. Le but de ces tests était de quantifier l'effet de la température sur le comportement général de la résine époxy pour ensuite fixer les niveaux de contrainte et de température à utiliser durant les essais de fluage.

Des essais de fluage-recouvrance furent ensuite effectués à 25, 50 et 70°C. Trois niveaux de contrainte (5, 10 et 15 MPa) furent testés pour chaque température. L'histoire de chargement appliquée consistait en une période de fluage de deux heures suivie d'une période de recouvrance de huit heures.

6. Développement de la loi de comportement et analyse des approches d'obtention des paramètres du modèle

Le PSTT fut appliqué à la partie fluage des courbes de fluage-recouvrance générées dans cette étude. Ainsi, les courbes de fluage furent latéralement déplacées sur une échelle de temps logarithmique afin d'obtenir, approximativement, une courbe de fluage maître pour chaque niveau de contrainte. La température ambiante fut choisie comme température de référence. Puisque l'étude n'utilisait seulement que quelques niveaux de température et que les tests étaient effectués sur une courte période de temps, les courbes ne se superposaient pas de manière à former une courbe maître sans ambiguïté. L'approche fut néanmoins utile pour valider que la résine étudiée présentait un comportement thermorhéologiquement complexe.

La réponse mécanique de la résine fut ensuite modélisée à l'aide d'un nouveau modèle de type Schapery. Diverses approches ont été étudiées afin de vérifier que l'utilisation des his-

toires complexes en contrainte et température pourrait aider à obtenir de meilleurs modèles constitutifs.

Les paramètres du modèle furent d'abord obtenus en utilisant des données provenant de tests isothermes de fluage-recouvrance à différentes températures et niveaux de contrainte. Le modèle obtenu fut ensuite utilisé afin de prédire la réponse du matériau dans des conditions thermomécaniques complexes. Les résultats démontrèrent une bonne concordance entre les prédictions du modèle et les résultats expérimentaux. Ainsi, une modélisation basée sur des courbes de fluage-recouvrance obtenues dans des conditions isothermes, combinée à l'utilisation du simple modèle non linéaire viscoélastique introduit dans cette étude permettait une bonne prédiction du comportement thermomécanique général de la résine époxy. Toutefois, l'utilisation de cette approche conventionnelle pour obtenir les paramètres du matériau à partir des courbes de fluage de recouvrance nécessite un travail laborieux.

Dans un deuxième temps, les paramètres du modèle furent obtenus à partir des données provenant à la fois de tests de fluage-recouvrance isothermes et d'histoires complexes de contraintes et de températures. L'étude démontra que l'ajout de données expérimentales obtenues dans des conditions de chargement transitoires en contrainte et en température ne put conduire à une amélioration significative des prédictions du modèle. Puisque cette dernière approche utilisait des données expérimentales plus réalistes pour la modélisation des propriétés de la résine, une meilleure représentation de la réponse thermomécanique du matériau était attendue.

Ces résultats ont donc évoqué la possibilité que le modèle utilisé dans cette étude puisse présenter certaines limites à caractériser le comportement de la résine époxy. De meilleures théories constitutives sont présentes dans la littérature pour modéliser le comportement thermomécanique des matériaux viscoélastiques. Ces théories nécessitent toutefois l'utilisation de

données expérimentales provenant de tests mécaniques plus élaborés afin de bien définir certaines des propriétés des matériaux, tel que le coefficient d'expansion thermique. Dans cette étude, celui-ci fut tout simplement considéré constant, ce qui a pu conduire à certaines divergences dans les réponses du modèle.

Dans la loi de comportement utilisée, la forme des fonctions non-linéarisantes fut arbitrairement exprimée comme étant quadratiquement dépendante de la contrainte et de la température. D'autres expressions moins restrictives auraient pu être plus représentatives de la dépendance en contrainte et en température. De plus, les fonctions obtenues ne présentaient pas un comportement monotones dans la plage de contrainte et de température analysée, ce qui pourrait être difficile à justifier physiquement.

Une nouvelle approche fut ensuite considérée afin d'obtenir les paramètres du matériau. L'approche consistait à utiliser l'information provenant des histoires complexes de chargement en contrainte et température afin de définir l'ensemble des paramètres du modèle. L'approche fut validée en comparant les données expérimentales et les prédictions du modèle ainsi obtenues pour des essais de fluage-recouvrance à différentes températures et niveaux de charge. Une différence notable fut obtenue. Ces résultats ont suggéré la possibilité que l'histoire de contraintes et de température utilisée ne présentait pas suffisamment d'informations sur le comportement du matériau pour adéquatement définir ses propriétés viscoélastiques. L'histoire thermomécanique utilisée dans cette étude présentait de courtes périodes de fluage et des rampes de chargement en contrainte et en température relativement rapides. L'utilisation d'histoires de chargement plus complexes présentant des rampes en contrainte et en température plus longues et plus lentes pourrait éventuellement aider à obtenir de meilleures prédictions. En dépit de la divergence notée entre les courbes prédites et les données expérimentales, l'approche a démontré un potentiel significatif pour la caractérisation des matériaux polymères en utilisant une quantité limitée de données expérimentales.

7. Conclusion et recherches futures

En conclusion, les principales contributions de cette étude sont les suivantes :

1. Le développement et l'installation d'un montage expérimental pour conduire des essais de traction mécaniques à haute température sur des échantillons polymères.

2. L'introduction d'un nouveau modèle viscoélastique non linéaire simple dépendant de la température et de la contrainte pouvant être utilisé pour modéliser le comportement thermomécanique des résines polymères

3. L'introduction d'une nouvelle approche visant à utiliser une quantité limitée de données expérimentales afin de définir l'ensemble des paramètres d'un modèle viscoélastique. Cette approche pourrait présenter un intérêt considérable pour réduire le temps et les ressources nécessaires afin de développer une loi de comportement thermomécanique.

Sur le plan expérimental, les recherches futures considèreront l'automatisation du contrôle de la température et du taux d'échantillonnage. Du côté de la modélisation, les prochaines recherches miseront sur l'utilisation de fonctions non-linéarisantes physiquement admissibles et sur l'amélioration des algorithmes d'optimisation utilisés pour trouver les paramètres du matériau. Enfin, il serait intéressant de poursuivre théoriquement et expérimentalement l'analyse introduite dans ce travail afin d'élaborer des tests optimaux visant à obtenir l'ensemble des paramètres thermomécaniques d'un matériau en utilisant une quantité réduite d'essais mécaniques.

CONTENTS

LIST OF TABLES

LIST OF FIGURES

LIST OF ACRONYMS AND ABBREVIATIONS

ASTM   American Society for Testing and Material

CRIAQ   Consortium for Research and Innovation in Aerospace in Quebec

CTE   Coefficient of Thermal Expension

DMA   Dynamic Mechanical Analysis

FD   Finite Difference

PMCM   Polymer Matrix Composite Materials

PWC   Pratt and Whitney Canada

RRC   Rolls Royce Canada

TCM   Thermorheologically Complex Material

TSM   Thermorheologically Simple Material

TTSP   Time-Temperature Superposition Principle

LIST OF SYMBOLS

α	Coefficient of thermal expansion
α_S	Coefficient of thermal expansion of the gage substrate
α_G	Coefficient of thermal expansion of the gage grid
a_i	Scalar functions
$\mathbf{A}^{(1)}$, $\mathbf{A}^{(2)}$ and $\mathbf{A}^{(3)}$	Internal matrices
γ	Temperature dependent parameter
Γ	Temperature coefficient of resistance of the grid conductor
D	Compliance
$\boldsymbol{D}^{(0)}$	Elastic compliance matrix
$\boldsymbol{\delta}$	Kronecker's delta
$\boldsymbol{\Delta\alpha}$	Vector of coefficients of thermal expansion
ΔEm	Output voltage of the Wheatstone bridge
$\boldsymbol{\Delta}S$	Transient compliance matrix
ε	Strain
E	Relaxation modulus
ζ	Integration variable
G_0	Elastic potential
g_i	Nonlinearizing functions
η	Stress dependent parameter
θ	Effective time
κ	Shift factor
K_t	Tranverse sensibility
λ_m	Inverse of the retardation times
ν_0	Poisson's ratio of the material used for calibrating the gage factor

$\boldsymbol{\xi}$	Vector of hidden variables
ρ	Stress dependent parameter
R	Resistance
σ	Stress
S_G	Gage factor
t	Time
T	Temperature
T_g	Glass transition temperature
T_R	Reference temperature
T_{TC}	TC reference temperature
T_{Test}	Test temperature
TC	Percent variation in gage factor with the temperature T_{TC}
ϕ	Stress energy function
Φ	$T - T_R$
V	Excitation voltage of the bridge
ψ	Ouput of a single Wheatstone bridge resistive arm
ω	Temperature dependent parameter
Ω	Reduced time

CHAPITRE 1

INTRODUCTION

The use of Polymer Matrix Composite Materials (PMCM) in the aerospace industry for the replacement of metallic components has steadily increased in the last decade. The principal advantage of such replacement is the reduction in the mass of the vehicle, which leads to fuel economies.

Of particular interest are the components close to the engines where the service temperature can reach $288°C$ ($550°F$). At this temperature, PMCM are likely to exhibit viscoelastic behavior. In addition, the combined effects of high temperature and the environment near the engines are likely to increase the aging process of the polymer matrix. Realistic characterizations of polymers have to take into account all these effects and use representative experimental data for defining constitutive models that accurately predict the material response under thermo-mechanical loading conditions.

For both structural and non-structural applications, the integration of polymeric materials for high in-service temperature components represents a serious challenge for aerospace companies. This motivated the creation of a collaborative project between universities and the industry. This project, supported by the collaborative Consortium for Consortium for Research and Innovation in Aerospace in Quebec (CRIAQ), Rolls Royce Canada (RRC) and Pratt and Whitney Canada (PWC), aims at developing novel methodologies for predicting the mechanical behavior of high temperature PMCM, which take into account static loadings, fatigue life as well as aging effects. The project focuses particularly on the behavior of an innovative polyimide resin, manufactured by Maverick Corporation, which was selected for its excellent high-temperature performance and processing versatility.

The current study is part of this collaborative research program. The work mainly addresses two objectives, namely the development of an experimental setup for testing polymers at high temperature and the elaboration of a stress-dependent and temperature-dependent constitutive theory for an epoxy resin. The study verifies the accuracy of using a nonlinearly viscoelastic model with parameters obtained from isothermal creep and recovery tests to predict the general strain response of polymers under complex stress and temperature histories. Various approaches are also studied to verify that the use of complex stress and temperature histories could help obtaining reliable models with limited testing.

This document is organized as follows : Chapter 2 presents a comprehensive review of the influence of temperature on polymer viscoelastic behavior together with common viscoelastic characterization techniques and testing methodologies. Based on the background presented in Chapter 2, Chapter 3 presents the rationale and sub-objectives of the project. Chapter 4 details the development of the experimental setup for testing polymer material at high temperature. The scientific approach and the relationship between the research objectives and the publications resulting from the thesis work are described in Chapter 5. In Chapter 6, modeling and experimental material parameters identification of a nonlinearly viscoelastic epoxy resin subjected to thermo-mechanical loading are presented in the form of a research paper. Experimental tests results and model predictions are then presented and discussed. Evaluation of the experimental setup and of the method for determining the parameters of the behavior law are discussed in Chapter 7. The conclusions of this work and future research are presented in Chapter 8.

CHAPITRE 2

LITERATURE REVIEW

2.1 Intuitive description of a viscoelastic material behavior

The behavior of a viscoelastic material is conventionally characterized by the nature of its response to two particular types of mechanical tests : creep-recovery and relaxation tests. Creep and recovery tests study the strain response of a material subjected to a constant stress σ_0 up to a time t_1. After t_1, the load is removed. As illustrated in Figure 2.1a, a viscoelastic material will present an instantaneous elastic deformation ε_0 at time $t_0 = 0$. The strain increases steadily up to ε_1 at t_1. Upon stress removal, the strain drops to ε_2. In the case of a linearly viscoelastic material, this instantaneous restoration $(\varepsilon_1 - \varepsilon_2)$ is equal to ε_0. Subsequently, the deformation decreases gradually until the material is restored to its original state. The creep part of the test provides the creep compliance $D(t)$ defined as

$$\varepsilon(t) = D(t)\sigma_0 \text{ (during the creep part)} \tag{2.1}$$

The relaxation test explores the variation of the stress in the material when imposing a constant strain ε_0 over a period of time t_1. Figure 2.1b schematizes the viscoelastic response for a relaxation test. An instantaneous stress σ_0 firstly appears when applying the strain at time $t_0 = 0$. Then, the material follows a progressive stress relaxation until it reaches a plateau value of σ_1. The relaxation test provides the relaxation modulus defined as

$$\sigma(t) = E(t)\varepsilon_0 \tag{2.2}$$

As can be seen, time is an important factor to consider in viscoelasticity. The response of a viscoelastic material is therefore influenced by the whole load history. For example, tensile

(a) Creep and Recovery test
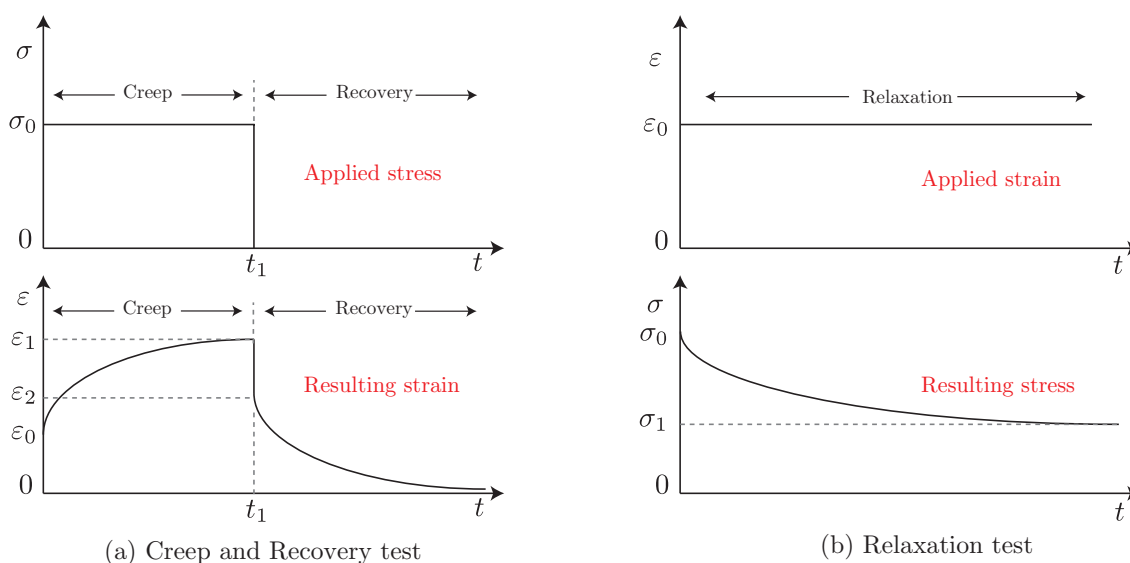
(b) Relaxation test

Figure 2.1 Schematic response of a viscoelastic material submitted to a creep-recovery test (a) and a relaxation test (b)

tests up to a given stress but for different strain rates might lead to different maximum stresses, as illustrated in Figure 2.2.

2.1.1 Influence of the temperature on polymer mechanical behavior

Temperature influences the mechanical behavior of viscoelastic polymers. Its effects can be explained by considering all active deformation mechanisms in the material at the microscopic scale. When the temperature is high enough, the available thermal energy can allow the relative motion of molecular chains inside the material. The creep and relaxation responses of polymer materials are consequently greatly affected by temperature changes. Figure 2.3 schematically shows the effect of temperature on the viscoelastic response of PMR-15 polyimide resin subjected to creep and recovery tests. It can be seen that for the same level of stress, higher temperatures will normally induce greater strains. Moreover, for high stress levels, the combined effects of stress and temperature might induce a nonlinearly viscoelastic behavior.
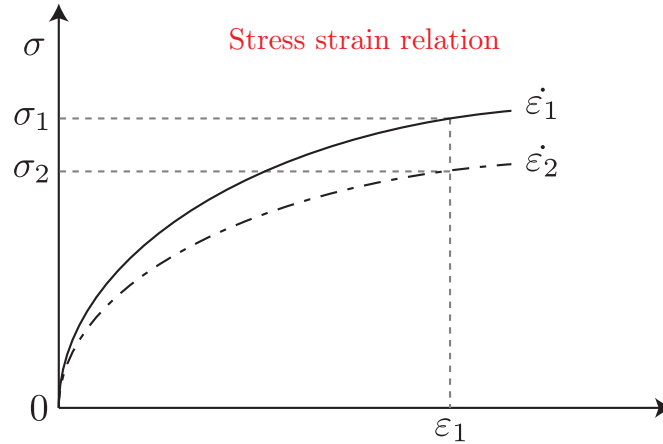
Figure 2.2 Schematic uniaxial response of a viscoelastic material submitted to different constant uniaxial strain rates. For higher strain rates ($\dot{\varepsilon}_1 > \dot{\varepsilon}_2$), greater stresses are induced to the material.

When a polymer material is heated progressively from a very low to a high temperature, the material passes from a rigid and brittle glassy state to a compliant rubbery state. The transition between the glassy and rubbery behavior of a polymer is characterized by the glass transition temperature (T_g).

The mechanical properties of a polymer rapidly drop close to T_g. The use of polymers is therefore conventionally done at temperatures approximatively 50°C below T_g. Since most of thermosetting resins have a glass transition temperature below 150°C, the use of polymers and polymer matrix composites for high temperature applications represents a significant challenge.

Table 2.1 shows the glass transition temperature for some common thermosetting resins. As can be seen, polyimide resins have a particularly elevated T_g. Due to their strong intermolecular bonds, this type of thermosetting resin can withstand much higher temperatures than most polymers and present therefore an interesting alternative to metal alloys for certain
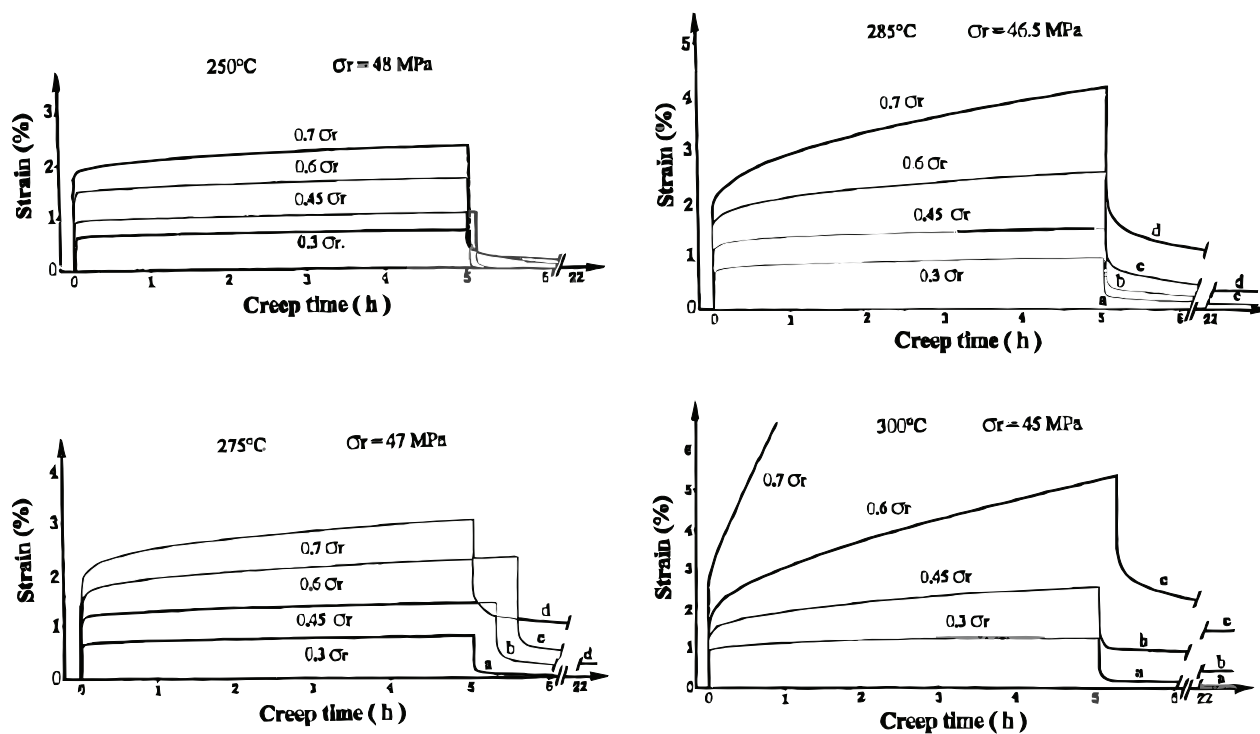
Figure 2.3 Influence of the temperature on the viscoelastic behavior of a polymer resin during creep-recovery tests. The Figure presents creep and recovery curves obtained by Marais, C. and Villoutreix, G. (1998) for the PMR-15 polyimide resin under various temperatures and stress levels. For an equivalent level of stress, higher temperatures induce greater strains. Moreover, for important loadings, the combined effect of both temperature and stress amplify the strains induced to the material and clearly generates a nonlinearly viscoelastic behavior.

niche applications.

2.2 Experimental methods for characterizing the thermo-mechanical behavior of a viscoelastic material

2.2.1 Standard test methods and problems

Mechanical testing aims at quantifying various phenomena that rule the behavior of a material. The approach measures the stress or strain response of the material under variations of some experimental variables controlled during the test. Mechanical tests allow the essential information on the material behavior gathered for defining the constitutive equation parameters. The accuracy and reliability of the data collected during the experimentations are therefore critical to obtain a representative constitutive law for the material.

The thermomechanical characterization of a polymeric resin inevitably requires an analysis of the material response under various temperature histories. In order to obtain the temperature effect on creep or relaxation responses, mechanical tests are generally performed at multiple constant temperatures and stress levels. A furnace or an environmental chamber is therefore required to carry out the experiments. Under such conditions, conventional mechanical tests present some difficulties.

Table 2.1 Glass transition temperature for some common polymers (Hoa (2009),Wilkes, C.E. *et al.* (2005))

Polymer	T_g ($^\circ C$)
Polystyrene	100
Polyvinylchloride	87
Polycarbonate	150
Nylon 6,6	57
Polyester	69
gathe d Epoxy	50-150
High temperature Epoxy	<260
Polyimide	250-370

First, measurement of the strain induced during testing becomes more complicated at elevated temperatures. The use of strain gauge requires special attention since the acquired signal during a test is disturbed by certain phenomena, such as the expansion of the grid, the deformation of the bonding adhesive, thermal expansion of the material and the variation of the gauge resistance. Other parasitic effects of thermal origins such as the thermal zero strain drift or the variation of strain gauges sensibility should also be considered. For the case where four equivalent resistances are used in the Wheatstone bridge illustrated in Figure 2.4, the output of the bridge can be approximated by (Vishay (2007))

$$\Delta Em = \frac{V}{4}(\psi_1 - \psi_2 + \psi_3 - \psi_4) \tag{2.3}$$

where the output of each strain gauge in the bridge can be expressed as

$$\psi = \left(\frac{\Delta R}{R}\right)_\sigma + \left(\frac{\Delta R}{R}\right)_{T/O}$$

$$= S_G \varepsilon + \left[\Gamma + S_G \left(\frac{1 + K_t}{1 - \nu_0 K_t}\right)(\alpha_S - \alpha_G)\right]\Delta T \tag{2.4}$$

where $\left(\frac{\Delta R}{R}\right)_\sigma$ and $\left(\frac{\Delta R}{R}\right)_{T/O}$ represent respectively a unit change from the initial reference resistance R caused by a stress σ and a change in temperature T. Γ is the temperature coefficient of resistance of grid conductor, S_G is the gauge factor of the strain gauge, K_t is the transverse sensitivity of the strain gauge, ν_0 is the Poisson's ratio of the material used for calibrating the gauge factor (0.285), $(\alpha_S - \alpha_G)$ is the difference between thermal coefficients of the substrate and the grid respectively and ΔT represents the temperature change from an arbitrary reference temperature. The strain gauges are conventionally designed to be used in a limited range of temperatures where the influence of thermal changes are minimized. As illustrated in Figure 2.5, some self-temperature-compensated strain gauges, such as Constantant alloy strain gauges, are designed in order to minimize the thermal output over a large
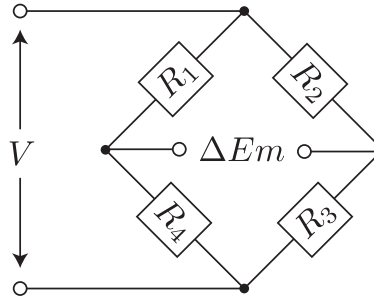
Wheatstone Bridge

Figure 2.4 Schematic representation of a Wheatstone bridge

range of temperatures. These gauges are normally provided with a fifth order polynomial equation characterizing the thermal output curve. This equation can be used to eliminate the temperature effect on the strain gauge only if the material to test is the same as the reference material used for defining the equation. In theory, it is possible to eliminate the thermal output of strain gauges by using a suitable arrangement of the Wheatstone bridge even if the material. When employing an active strain gauge bonded on the specimen and a second stress-free strain gauge which perceives the same temperature, the two strain gauges can be connected in an adjacent arm (positive and negative) of a half bridge configuration to compensate their thermal output. It is however technically difficult to apply an equivalent temperature history to both strain gauges during the whole duration of a test.

Another alternative is to measure the deformation using an extensometer. Its use is nonetheless laborious at high temperature. It must be able to both undergo the temperature range tested and to fit inside the oven or the environmental chamber. Since the output signal of extensometers is achieved through a full bridge configuration, similar problems to that of strain gauges may also exist when they are exposed to temperature. Certain types of high temperature extensometers are however designed in order to read the strain through a me-
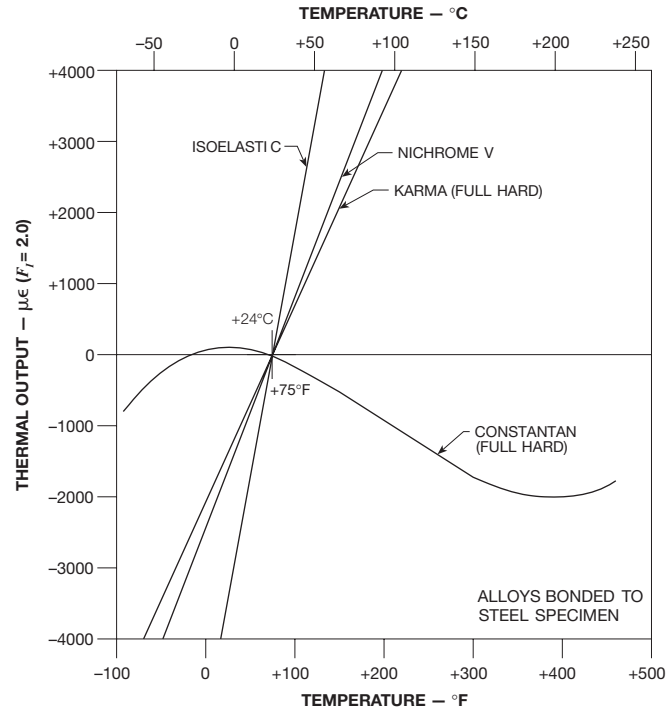
Figure 2.5 Thermal output variation with temperature for several strain gauge alloys bonded to steel (Vishay (2007)).

dium connected to the specimen while staying outside the furnace.

Temperature control during testing is also very important. Achieving a uniform temperature in the test section is a considerable challenge. In general, furnaces use heating elements to warm the air surrounding the specimen. The control of the temperature is usually done by using thermocouples located near the heating elements. It is not unusual that there is difference between the temperature read by the thermocouples and that of the material. Due to natural convection, the upper portion of the furnace is also generally warmer than the lower portion. In addition, the thermal capacitance difference between air and polymers leads to some thermal inertia during a temperature ramp. Even after reaching a steady state, the air surrounding the sample is rarely at a uniform temperature and the temperature in the specimen test section is consequently difficult to control.

Environmental chambers offer a better accuracy and a better control of the temperature than furnaces. Some chambers benefit from a mechanical convection system ensuring the uniform distribution of heat deployed by the heating elements throughout the interior of the heated enclosure. The temperature chambers are much more expensive than traditional ovens. They require the use of special mechanical grips that must be inserted into the chamber. With these systems, the use of hydraulic grips is problematic because the oil flowing in the system is also subjected to the same temperature.

Figure 2.6 presents a schematic representation of an experimental setup using an environmental chamber (a) and a furnace (b). As can be seen, another difficulty comes from the fact that samples are not accessible during testing and it might be difficult to adjust some settings once a test is started. In addition, failure of a sample may cause a burst of the material, which can damage components of the furnace or the environmental chamber.

2.2.2   Complex tests and methods

In most of the approaches that have been suggested to date, material parameters are normally obtained by isothermal creep and recovery tests (Lou et Schapery (1971), Zaoutsos *et al.* (1998), Papanicolaou *et al.* (1999), for example). Tests are usually performed at a fixed temperature and then repeated to completely cover the range of temperatures required. However, this experimental approach for obtaining the temperature and stress dependence parameters of the models might not truly represents the thermo-mechanical behavior of the material subjected to complex in-service loadings and temperature histories.

Several studies investigated polymer responses under time-varying uniaxial load histories at room temperature. For example, G'sell et Jonas (1981) studied the stress response of seven common thermoplastics subjected to various tests under true strain control at room temperature. Transient strain rates were used during the experiments, interrupted by re-

(a) Environmental chamber   (b) Furnace
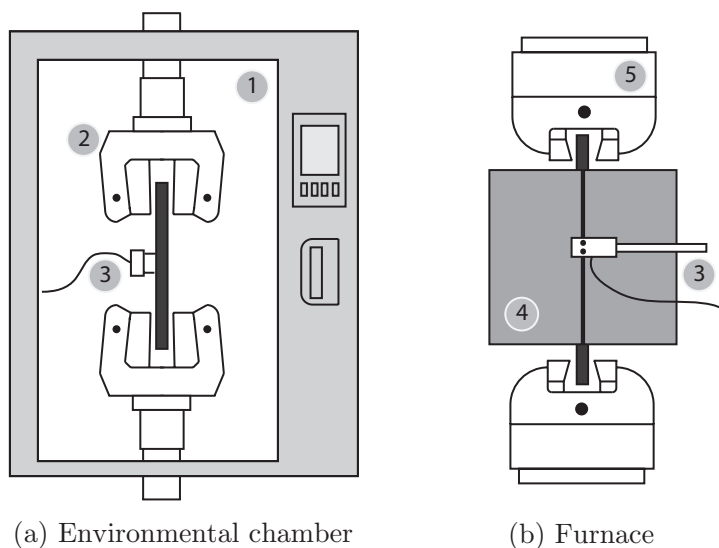
Figure 2.6 Schematic representation of an experimental setup using an environmental chamber (a) and a furnace (b). (a) High temperature mechanical grips (2) have to be inserted inside the environmental chamber (1) as well as the extensometer (3). (b) The hydraulic grips (5) stand outside the furnace (4) as well as the extensometer (3).

laxation periods. Peretz et Weitsman (1982) studied the nonlinearly viscoelastic behavior of FM-73 adhesive. Standard creep and recovery tests were used to obtain the material properties for the model. The accuracy of the model was then verified by two-step creep tests and loading-unloading experiments. Nordin et Varna (2005, 2006) compared the use of one-step and two-step loadings and unloadings for obtaining the parameters of a Schapery's nonlinear viscoelastic model. The studies showed that the usage of two-step loadings for predicting the behavior of vinyl ester and paper composites leads to more accurate results. Lévesque *et al.* (2008) introduced an experimental procedure which considers the whole mechanical response of a polymer. The approach did not rely on creep and recovery tests. Complex loading and unloading paths were designed for accurately identifying the isothermal nonlinearly viscoelastic behavior of a thermoplastic. The results demonstrated the importance of using various loading histories to validate the accuracy of the models. Dreistadt *et al.* (2009) proposed a characterization procedure for polycarbonate using repeated loading-unloading tests at dif-

ferent strain and stress levels, interrupted by periods of creep.

Similar studies for elevated isothermal temperatures were also conducted. Ruggles-Wrenn et Balaconis (2008) investigated the influence of the stress-rate on the behavior of BMI 5250-4 at 191°C. The effect of loading rate was studied with loading and unloading tests under various constant stress rates. The effect of prior loading history was explored through stepwise creep tests incorporating loading and unloading stress ramps with intermittent creep periods at several stress levels. Results showed that the creep response was significantly affected by the prior stress rate and prior loading history. The nonlinearly viscoelastic model used could hardly predict creep responses and loading-unloading behavior, especially for low loading rates. Falcone et Ruggles-Wrenn (2009) repeated the study on PMR-15 thermosetting polyimide at 288°C with similar conclusions. McClung et Ruggles-Wrenn (2008) characterized the effect of prior strain rate and prior strain rate history. Various complex strain histories incorporating intermittent relaxation periods at several strain levels were realized at 288°C on PMR-15. They obtained the same conclusions as that of Ruggles-Wrenn et Balaconis (2008).

Rather than conducting isothermal testing for studying the influence of temperature, Peretz et Weitsman (1983) extended their work on nonlinearly viscoelastic behavior of FM-73 adhesive to incorporate the effect of temperature on the mechanical response. Creep and recovery experiments were carried out for several temperatures with the integration of a cool down to 30°C when removing the stress for the recovery period. Various levels of creep stresses under the influence of a constant temperature ramp were applied to validate the nonlinear model used. Ohashi *et al.* (2002) studied the response of polypropylene under transient temperatures. Compressive stress-strain curves were obtained under trapezoidal temperature waveforms. Harper et Weitsman (1985) summarized a methodology used to characterize time-temperature behavior of a thermorheologically complex material (by opposition to a thermorheologically

simple material, see section 2.3.2). The study concluded that using combined results from isothermal creep tests and complex transient temperature experimentations led to a greater correspondence between experimental results and model predictions.

2.3 Modeling of a viscoelastic material

2.3.1 Linearly viscoelastic constitutive model

The general strain response of a linearly viscoelastic material can be expressed as (Lévesque *et al.* (2008))

$$\varepsilon_i(t) = -\frac{\partial G_0}{\partial \sigma_i} + \int_0^t \sum_{m=1}^M S_{ij}^{(m)}(1 - \exp[-\lambda_m(t - \tau)])\frac{\mathrm{d}\sigma_j}{\mathrm{d}\tau}\mathrm{d}\tau \tag{2.5}$$

where $-\frac{\partial G_0}{\partial \sigma_i}$ represents the linearly elastic response while the second term represents the viscoelastic response. $S_{ij}^{(m)}$ are positive semi-definite matrices and λ_m are the so-called retardation times.

As stated by Findley *et al.* (1989), two conditions have to be satisfied for a material to exhibit a linearly viscoelastic behavior. The first condition is the proportionality and implies that the strain history response due to a stress history $\sigma^{(1)}(t)$ corresponds to β times the strain history response induced by a different stress history $\sigma^{(2)}(t) = \beta\sigma^{(2)}(t)$, where β is a scalar multiplicative factor.

Then, let $\varepsilon^{(1)}(t)$ and $\varepsilon^{(2)}(t)$ be the strain responses to the stress histories $\sigma^{(1)}(t)$ and $\sigma^{(2)}(t)$. Let $\sigma^{(3)}(t) = \sigma^{(1)}(t) + \sigma^{(2)}(t)$. The second condition is so-called superimposition and states that the stress response to $\sigma^{(3)}(t)$, expressed by $\varepsilon^{(3)}(t)$, is given by : $\varepsilon^{(3)}(t) = \varepsilon^{(1)}(t) + \varepsilon^{(2)}(t)$. The proportionality and superimposition requirements are respectively illustrated in Figures 2.7 (a) and (b).

Most materials exhibit a linear response over certain ranges of stress and temperature. The use of a linear model might predict the behavior of a material in certain conditions but is not necessarily adequate for all load histories. When requirements of the design exceed the limits of the linear model, nonlinearly viscoelastic models can lead to more accurate results.

2.3.2 Time-Temperature Superposition Principle

The effect of the temperature on the viscoelastic behavior of polymers has been widely studied by means of the Time-Temperature Superposition Principle (TTSP) (Luo (2007), Olasz et Gudmundson (2005), Zhao (2008), for example). The concept implies that relaxation times, which are temperature-dependent, can be related to those at a reference temperature by a simple multiplicative shift factor. The TTSP uses the effective time concept to characterize the effect of the temperature on the response of viscoelastic materials. The effective time (θ) can be defined by noting that all relaxation that occurs over an infinitesimal period of time $\mathrm{d}t$ at temperature T is $\kappa(T)$ times of that occurring at a reference temperature T_R over a time period $\mathrm{d}\theta$ (Brinson et Gates (2000)), so that

$$\theta(t) = \int_0^t \kappa(T(\zeta), \zeta)\mathrm{d}\zeta \tag{2.6}$$

where $\kappa(T)$ is called the temperature shift factor. Basically, the method consists of replacing the time variable in the material strain response by θ computed by means of Equation (2.6). By extrapolating the experimental data of various temperatures, the concept allows to set a single master curve which is representative of the material behavior for a specific stress state and temperature. If the temperature is kept constant over time, it can be seen that Equation (2.6) can be simplified as

$$\theta(t) = \kappa(T)t \tag{2.7}$$
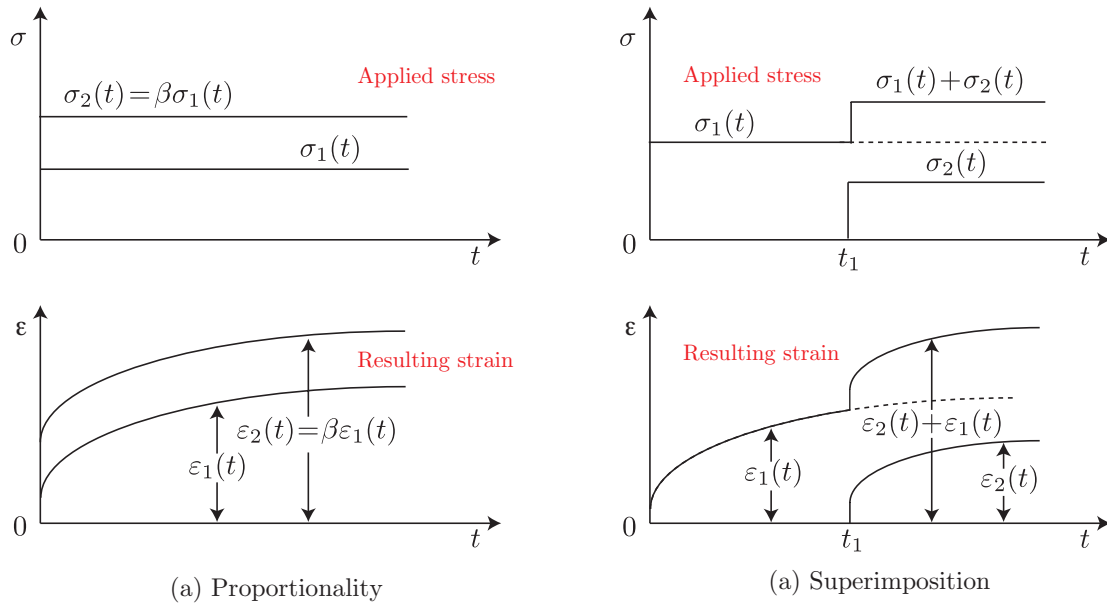
Figure 2.7 Schematic representation of proportionality (a) and superimposition (b) concepts. Figure is inspired from Findley *et al.* (1989)

On a logarithmic time scale, the principle corresponds to a simple lateral displacement of the experimental curves. Consider a relaxation test performed at a constant temperature $T_1 > T_2$ as illustrated in Figure 2.8. Based on this theory, it can be seen that shifting horizontally the curve associated with T_1 by a factor of $\log \kappa_T$ allows to reproduce the curve associated with T_2.

One main application of the concept consists of predicting long-term creep responses of polymers using short time tests (Ohashi *et al.* (2002), Olasz et Gudmundson (2005), Zhao (2008), Luo (2007), for example). Materials that can be fully characterized by means of the TTSP are categorized as Thermorheologically Simple Material (TSM) while materials that do not obey the TTSP are called Thermorheologically Complex Material (TCM). TCM exhibit several time-temperature dependent mechanisms (Harper et Weitsman (1985)) and require more complex models such as Schapery's nonlinear model (Sawant et Muliana (2008), Muliana et
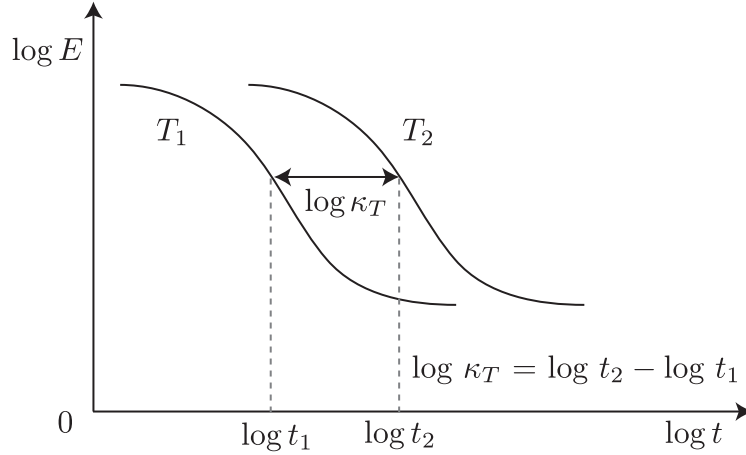
Figure 2.8 Schematic of Time-Temperature Superposition Principle. A relaxation test is achieved at a constant temperature $T_1 > T_2$ and is related to the behavior of the material for a temperature T_2 by rightward shifting on a logarithmic time scale the relaxation curve over a distance equivalent to $\log \kappa_T$

Khan (2007), Harper et Weitsman (1985), Muliana (2009)).

2.3.3 Schapery's constitutive theories

The hereditary integral

In thermodynamics of irreversible processes, the state of a material can be fully characterized by state function of state variables. These state variables are divided into observable variables (the stresses in our case) and hidden variables (labelled as $\boldsymbol{\xi}$, for which no physical sense is given at this time). Combination of the first and second principles of thermodynamics leads to the differential equations (Schapery (1997)) :

$$a_1(\sigma, T)B_{rs}\dot{\xi}_s + a_2(\sigma, T)A_{rs}^{(3)}\xi_s + a_3(\sigma, T)A_{jr}^{(2)}\sigma_j(\sigma, T) + a_1\beta_r\Phi = 0 \qquad (2.8)$$

and to the constitutive equation :

$$\varepsilon_i(t) = -a_4(\sigma, T)A_{ij}^{(1)}\sigma_j - \left(\frac{\partial a_3(\sigma, T)}{\partial \sigma_i}A_{js}^{(2)}\sigma_j + a_3(\sigma, T)A_{is}^{(2)}\right)\xi_s = 0 \tag{2.9}$$

where matrices $\mathbf{B}$ and $\mathbf{A} = \begin{bmatrix} \mathbf{A}^{(1)} & \mathbf{A}^{(2)} \\ \mathbf{A}^{(2)T} & \mathbf{A}^{(3)} \end{bmatrix}$ are positive semi-definite and symmetric, $\boldsymbol{\beta}$ is

a vector, $\Phi = T - T_R$ where T_R is the reference temperature, a_i are scalar functions of $\boldsymbol{\sigma}$ and

T and $(\dot{\ })$ denotes a time differentiation. Strains are obtained by solving Equation (2.8) for

$\boldsymbol{\xi}(t)$ and then replacing $\boldsymbol{\xi}$ in Equation (2.9). A reduced time is defined as

$$\Omega(t) = \int_0^t \frac{a_2(\chi)}{a_1(\chi)}\mathrm{d}\chi \tag{2.10}$$

and the strains can be expressed as

$$\begin{aligned}
\varepsilon_i(t) = \frac{\partial \varphi}{\partial \sigma_i} + \left(\frac{\partial a_3}{\partial \sigma_i}\sigma_j + a_3\delta_{ij}\right)\int_0^t \Delta S_{jk}\left(\Omega(t) - \Omega(\tau)\right)\frac{\mathrm{d}}{\mathrm{d}\tau}\left[\frac{a_3(\tau)}{a_2(\tau)}\sigma_k(\tau)\right]\mathrm{d}\tau \\
+ \int_0^t \Delta\alpha_i\left(\Omega(t) - \Omega(\tau)\right)\frac{\mathrm{d}\Phi(\tau)}{\mathrm{d}\tau}\mathrm{d}\tau
\end{aligned} \tag{2.11}$$

where δ_{ij} is Kronecker's delta and φ is a stress energy function associated with a nonlinearly

elastic material. $\boldsymbol{\Delta}S$ and $\boldsymbol{\Delta}\alpha$ are respectively the transient compliance matrix and the thermal

expansion vector which can be expressed as Prony series as

$$\Delta S_{ij}(t) = \sum_{m=1}^M S_{ij}^{(m)}\left(1 - \exp\left[-\lambda_m t\right]\right) \tag{2.12a}$$

$$\Delta\alpha_i(t) = \sum_{m=1}^M \alpha_i^{(m)}\left(1 - \exp\left[-\lambda_m t\right]\right) \tag{2.12b}$$

where $\mathbf{S^{(m)}}$ are positive semi-definite symmetric matrices and $\lambda_m \geq 0$ are the inverse of the

retardation times. In this study, the material was assumed to be isotropic and only axial

tests were performed on the specimens. If the Coefficient of Thermal Expension (CTE) is

assumed to be constant and independent of the temperature, $\Delta\alpha(t) = \alpha$. Therefore, the three-dimensional hereditary integral can be reduced to the stress-based uni-dimensional integral (Schapery (1969))

$$\varepsilon(t) = g_0 D^{(0)}\sigma(t) + g_1 \int_0^t \Delta S\left(\Omega - \Omega'\right) \frac{\mathrm{d}}{\mathrm{d}\tau}\left[g_2\sigma(\tau)\right] \mathrm{d}\tau + \alpha\Phi \qquad (2.13)$$

where $\mathbf{D}^{(0)}$ is the elastic compliance matrix and the $g_j(\sigma, T)$ are

$$g_0(\sigma, T) = a_4; \quad g_1(\sigma, T) = \frac{\partial a_3}{\partial \sigma}\sigma + a_3; \quad g_2(\sigma, T) = \frac{a_3}{a_2}; \quad g_3(\sigma, T) = \frac{a_1}{a_2}. \qquad (2.14)$$

2.4 Summary of the findings

The literature review highlighted the influence of the temperature on the viscoelastic behavior of polymer resins. It was seen that various techniques present in the literature allow establishing stress-dependant and temperature-dependant constitutive equations of polymers. Under particular temperature conditions for which the material behavior exceeds the limits of the linear range, the linearly viscoelastic model might lead to a poor representation of the material response. In this case, proper prediction of the material response can be obtained using the TTSP or Schapery's constitutive theories, whether if the material exhibits a typical thermoreologically simple or a complex material behavior.

On the experimental side, the definition of constitutive equations for a material is based on experimental data obtained from mechanical tests. Mechanical testing is however challenging at elevated temperature and requires particular equipment and procedures. The thermo-mechanical behavior of polymers is generally studied by performing multiple creep and recovery tests at various temperature and stress levels under isothermal conditions. Very few authors have explored the possibility of using general stress and temperature histories for obtaining material parameters.

CHAPITRE 3

OBJECTIVES AND RATIONALE OF THE PROJECT

The main purpose of this work is to study the thermo-mechanical response of a polymer resin under various stress and temperature histories. Based on the literature survey performed, two main aspects requiring attention were identified and led to the two objectives studied in this work, namely

1. The literature survey showed that mechanical testing at elevated temperature leads to some technical challenges. Measurements of the strain response and temperature control are two important elements to consider during testing. The first sub-objective consists therefore of developing an experimental setup for performing reliable and precise mechanical tests at high temperatures.

2. The literature survey showed that most of the existing studies did not use stress and temperature histories that are representative of the general behavior of the material to be characterized. Most of the tests are usually done for isothermal conditions. However, some studies demonstrated that using transient temperature and stress histories for determining the material parameters could lead to a better representation of the real material behavior. The second sub-objective of this study consists of verifying the accuracy of using isothermal creep and recovery data for determining the nonlinearly viscoelastic properties of a polymer resin and to predict the strain response of the material under complex stress and temperature histories.

CHAPITRE 4

DEVELOPMENT OF AN EXPERIMENTAL SETUP FOR PERFORMING MECHANICAL TESTS AT ELEVATED TEMPERATURE

4.1 Setup requirements

The development of the experimental setup for performing mechanical tests on polymers at elevated temperature had to follow certain requirements imposed by the project, namely

1. The setup had to be able to perform standard tensile and creep-recovery tests.

2. The setup had to be able to apply transient stress and temperature histories.

3. The setup had to be able to perform tests from room temperature up to 300°C.

4. The setup had to deliver precise strain, displacement and force measurements.

5. The temperature variation during the tests had to meet proper ASTM requirements.

6. The setup had to be able to continuously acquire and record the experimental data.

4.2 ASTM standards

Mechanical testing is generally ruled by standard practices. These practices set out the technical standards and methodology to use in order to ensure the validity of experimental results. The American Society for Testing and Material (ASTM) standards for conducting tensile and creep-recovery tests on polymer materials are :

– ASTM D638 : Standard test methods for tensile properties of plastics
– ASTM D621 : Standard test methods for tensile, compressive and flexural creep of plastics

These ASTM standards give some indications including specimen dimensions, the loading rate or strain to impose, the minimum acquisition rate for the acquisition and all the procedures to be followed while testing. These standards give guidelines for tests performed at room temperature. There is no specific ASTM guideline to be used for performing tensile tests or creep tests on polymer material at higher temperatures. However, some specific standards give general indications to consider in such conditions :

– ASTM D618 : Standard practice for conditioning plastic for testing

– ASTM E1319 : Standard guide for high-temperature static strain measurement

These standards have been considered throughout this project and the development of the experimental setup.

4.3   Setup description

The experimental setup developed for the project is presented in Figure 4.1. A MTS 653.04 high temperature furnace was prefered to an environmental chamber for performing the tests. The cost of an environmental chamber was at least four times that of the selected furnace and would have required the purchase of specific mechanical grips. The furnace was designed to cover a wide range of temperatures up to $1400°C$ and presented a center split design allowing an easy access of the specimen and the possibility to accommodate an high-temperature extensometer. Each side of the furnace was installed on a slide rail built into the load frame mounting support. The furnace was composed of three heated zones, independently controlled by a MTS 409.83 temperature controller and Type R thermocouples. The tests were carried out with a servocontrolled MTS 810 mechanical testing machine controlled by a MTS 458.20 controller from which complex test programs could be input by a MTS 458.91 MicroProfiler. The testing machine had a 250kN (55Klbs) load frame capacity and a 25kN (5.5Klbs) load cell was purchased in order to adapt the loading range of the testing machine for polymer testing. The controller cartridge used allowed a maximum accuracy of the load cell within the 0-5kN operating range. The load precision presented less than 1%
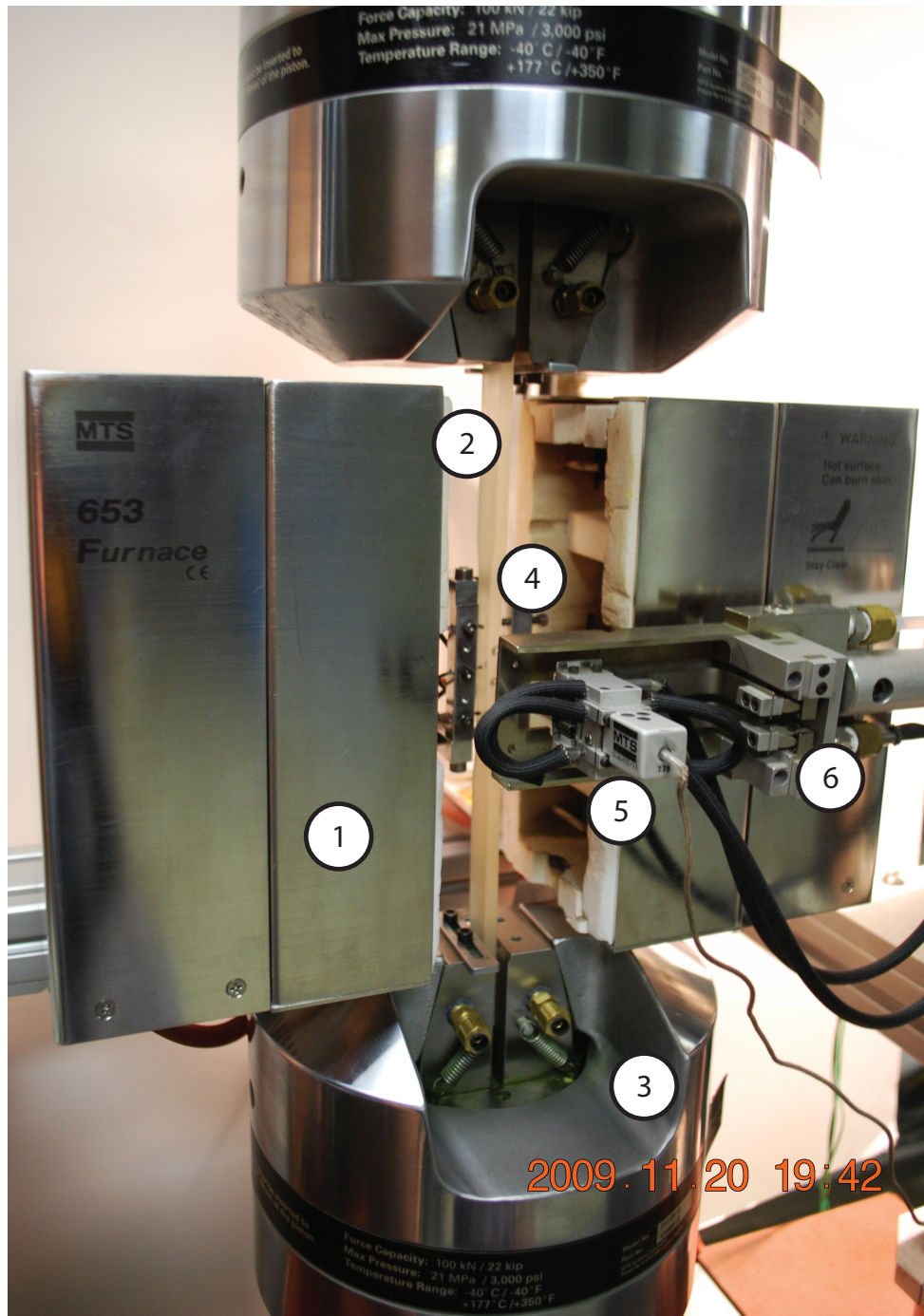
Figure 4.1 General view of the experimental setup. The two sides of the oven (1) are opened and an epoxy sample (2) is inserted into the grips (3). The special fixture (4) is attached to the specimen along with the extensometer (5). The extensometer is linked to the specimen by two quartz rods. The extensometer support (6) have a spring that keeps a little pressure on the extensometer in order to position the quartz rods on the specimen.

errors for loads greater than 50N.

The testing machine was equipped of MTS 647.01A hydraulic grips. Even if hydraulic grips stayed outside the furnace during the tests, heating conduction from specimens at high temperature still presented an issue. MTS 647.10 water-cooled wedges were therefore installed on the hydraulic grips to prevent damage when heating specimens. A flat wedge gripping surface with a Surfalloy finish was selected to provide firm gripping of polymers and composites without grip-induced failures. The wedges had alignment guides to ensure consistent side insertion for specimen thickness up to 7.6mm (0.3 inch).

An independent MTS 685 pump system allowed to control the hydraulic pressure inside the grips without affecting the general hydraulic system that controls the axial load on the specimen. The choice of a such system provided a better control of the load to apply on specimen during testing.

4.4 Strain measurement

Strains were measured using a MTS 632.42 high temperature extensometer that had a 0.5 inch gage length. The device was available in the laboratory and only required a calibration that was performed by a MTS technician before the beginning of the tests. The extensometer stayed outside the furnace during the tests and measured strains by mean of two quartz rods standing off the specimen. The quartz rods minimized thermal expansion errors and conduction losses from the specimen. A support system held the extensometer securely in place while allowing full movement of the extension rods. The deformation of the specimen was calculated according to the relative displacement of the quartz rods. The extensometer was water-cooled and could be used to measure deformation up to $1200°C$ with a resolution typically less than 0.15% of the cartridge travel range. The extensometer required a water flow rate of approximately 0.004 to 0.05 gpm (0.15 to 0.2l/min) of water below $35°C$.

Figure 4.2 shows the various quartz rods type that could be used with the high temperature extensometer. Basically, round rod type extensions are specifically designed for circular specimen so only flat and conical end type were therefore tested. Results showed that a better accuracy was possible with conic end rods because chisel-edge end type were recurrently slipping on the surface of the specimen. A close-up view of the high temperature extensometer and its extension rods is shown in Figure 4.3(b).

Vishay EA-06-125TM-350 strain gages were preferred to the extensometer for constant displacement rate tensile tests up to potential failure in order to avoid damaging the extensometer in case of specimen failure. The strain gages were bonded with Vishay M-Bond 200 adhesive. Two strain gages were used for each test and they were symmetrically bonded on both side of the specimen at the center axis. The strain gages were placed in the two positive branch of a Wheatstone half-bridge configuration to avoid parasitical effects induced by torsion and bending.

Since tensile tests were performed at a constant temperature, strain measurement could be made without compensating or correcting the thermal output (see Equations 2.4). The gage factor of the strain gages were however adjusted following the equation

$$S_G^* = S_G \left(\frac{TC}{100°C} \right) (T_{Test} - T_{TC}) = 2.115 \left(\frac{1.2\%}{100°C} \right) (T_{Test} - 24°C) \tag{4.1}$$

where TC represents the percent variation in gage factor with the reference temperature T_{TC} given on the gage package data label and S_G^* is the gage factor considering the temperature correction.
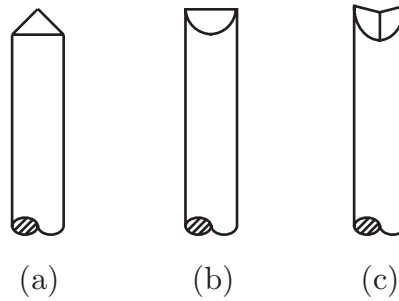
Figure 4.2 Various set of quartz extension push rod to be used with the high temperature extensometer. (a) conical point (b) chisel-edge (c) V chisel edge.

4.5   Temperature control

Temperature control was achieved by setting the temperature in the air surrounding the furnace heaters with the MTS controller while monitoring the specimen temperature with thermocouples. A specifically designed fixture for attaching the thermocouples was used in order to obtain a space-wise and time-wise uniform temperature in the test section. This apparatus could be easily clipped on the specimen and measured the variation of the temperature at three different positions evenly distributed over a 1.5 inches length. The fixture allowed easily controlling the temperature in the specimen gage length while ensuring a good precision. The concept of the fixture and the real device are shown in Figure 4.3.

Figure 4.4 presents an acquisition of the temperature realized at $50°$ for 10 hours. It can be seen that a $\pm 0.75°$C uniformity was obtained along the specimen gage length. This variation represented the maximum difference between temperatures read by the three thermocouples at any specific moment during a test. Moreover, each thermocouple reading remained within a $\pm 0.75°$C range during the tests. Acquisition of the temperature was conducted also for longer periods and at higher temperatures (up to $200°$C on BMI composite specimens) and comparable precision could be reached.
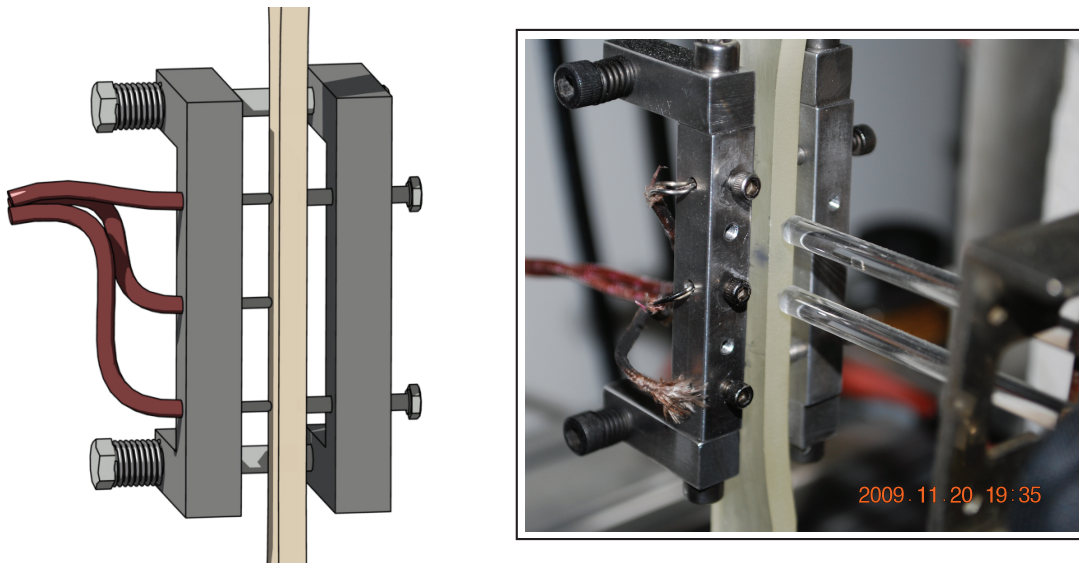
(a) Thermocouple fixture Concept

(b) Actual thermocouple fixture
along with the extensometer

Figure 4.3 Thermocouple fixture. The fixture allows the positioning of three thermocouples evenly distributed over a 1.5 inches length on the specimen surface. (a) Thermocouple fixture Concept (b) Actual thermocouple fixture along with the high temperature extensometer. The high temperature extensometer is installed perpendicularly to the thermocouples fixture and is linked to the specimen by two quartz rods that follow the deformation during the test.
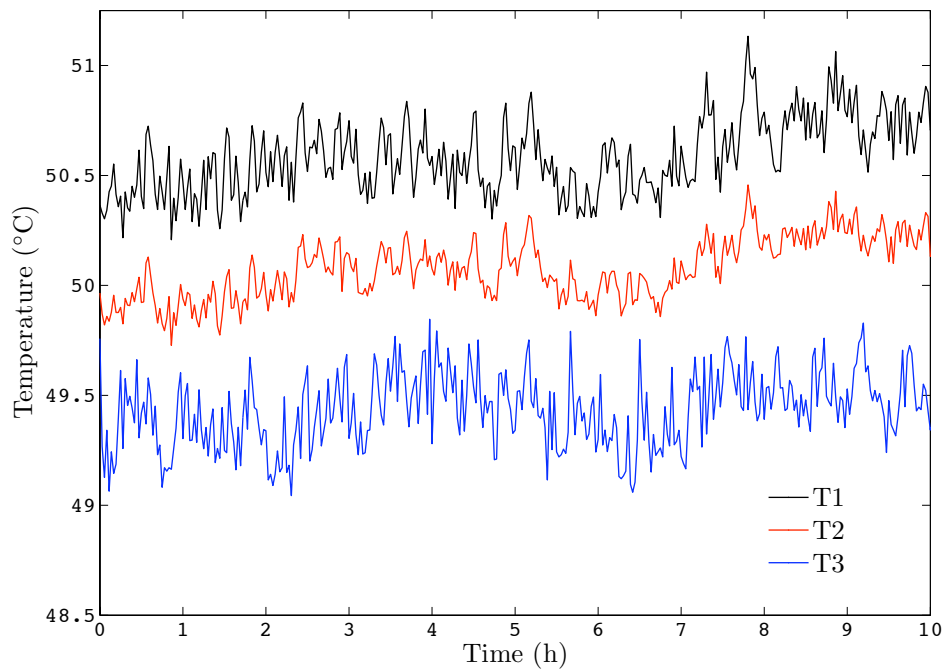
Figure 4.4 Temperature acquisition. The figure shows the acquisition of the temperature over a period of 10 hours at 50°C. It can be seen that a ± 0.75°C uniformity can be obtained along the specimen gage length. This variation represents the difference between temperatures read by the three thermocouples at a specific moment during a test. The variation of each thermocouple stays within a ± 0.75°C range along the duration of the tests.

4.6   Data Acquisition

The load, the displacement of the grips and the strain of the high temperature extensometer were recorded through a 16-bit resolution NI PCI-6221 acquisition card built in a computer. A NI 9237 module with a resolution of 24 bits recorded strain measurements from strain gages. Temperature signals from the thermocouple fixture were recorded by a 24-bit NI 9211 module specially developed for high-accuracy thermocouple measurements. Both modules were mounted on a CompactDAQmx NI-9172 chassis, which could accommodate up to eight different modules. The chassis CDAQ NI-9172 was then simply connected to the computer through a USB connectivity.

An acquisition program was developed in LabVIEW 8.5 software with the assistance of the technician, Mr. Benedict Besner. The program basically displayed the various signals and allowed controlling the acquisition frequency. Experimental data were then stored in a .txt file defined by the user.

CHAPITRE 5

METHODOLOGY

5.1 Material selection

At the time this Master thesis was performed, the polyimide matrix to be studied in the course of the collaborative project was not received. Another material had to be used. Since the essence of the general project is to develop the methodology for modeling and testing a polyimide resin at high temperatures, it is preferred that material selected in this study exhibits similar room temperature properties with the polyimide resin involved in the collaborative project.

The material had to be a low cost resin with a relatively high glass transition temperature (over at least 125°C) in order to allow for a certain range of temperature for testing. The epoxy system chosen consisted of an EPON 862 resin mixed with an Epikure 3300 (amine) curing agent at 24.8phr. The epoxy system was molded in rectangular flat molds and followed a cure schedule of 10 hours at room temperature, 1.5 hours at 82°C and 1.5 hours at 150°C. Thin wet films of Loctite Frekote 44-NC release agent were sprayed on the surface of the molds to facilitate the demolding process. The cure was done in a Blue M Electric 206 oven. Four panels of 10×15 inches and 3 panels of 8×12.5 inches were manufactured. Surfaces of the panels were then milled to fit the thickness tolerance indicated by the ASTM standard D638.

5.2 Specimen dimensioning

Specimen dimensioning was done following the ASTM standard D638, which allows essentially four types of flat specimens. The choice of specimen type was made in order to met

the general setup proportions. ATSM Type I specimens were used for all mechanical tests. Specimens were made long enough to allow an adequate gripping of the material outside the furnace. The distance between the grips defined by the standard could however not be respected due to the furnace dimensions.

Since room temperature tests did not necessitate the use of a furnace, length of room temperature specimens was set 0.5 inch shorter than that of high temperature specimens. Dimension of the specimens are given in Figure 5.1. Tensile testing specimens were obtained by waterjet cutting. Specimen dimensions were verified with an electronic caliper. A few specimens did not respect tolerances defined by the ASTM standard and were therefore not tested. Center axis guidelines were drawn on the specimens in order to facilitate their positioning inside the grips.

5.3 Material properties verification

The Coefficient of Thermal Expansion of the material was determined prior to testing. Two specimens were subjected to a temperature ramp of $1°$C/min while the thermal expansion of the material was measured with the high temperature extensometer. The curves obtained are presented in Figure 5.2. A thermal expansion coefficient of $0.004\% C^{-1}$ was determined according to a mean slope obtained from both curves. It was found to be relatively constant for the tests performed.

In order to determine the glass transition temperatures of the material, Dynamic Mechanical Analysis (DMA) tests were performed on the epoxy specimens. DMA is a thermal analysis technique that measures the properties of materials under a periodic sinusoidal stress. The phase difference between the stress and the resultant sinusoidal strain waves, together with the amplitudes of the stress and strain waves is used to determine a variety of fundamental material parameters, including storage and loss moduli. T_g of a resin can be determined by
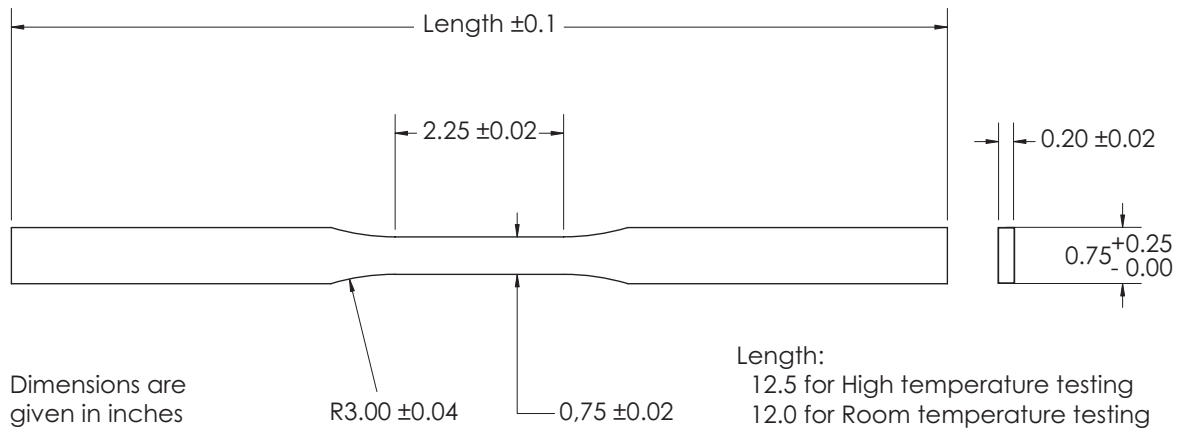
Figure 5.1 ASTM type I specimens used for tensile test and creep-recovery tests. Dimensions are given in inches. Two different lengths were used depending on the temperature.
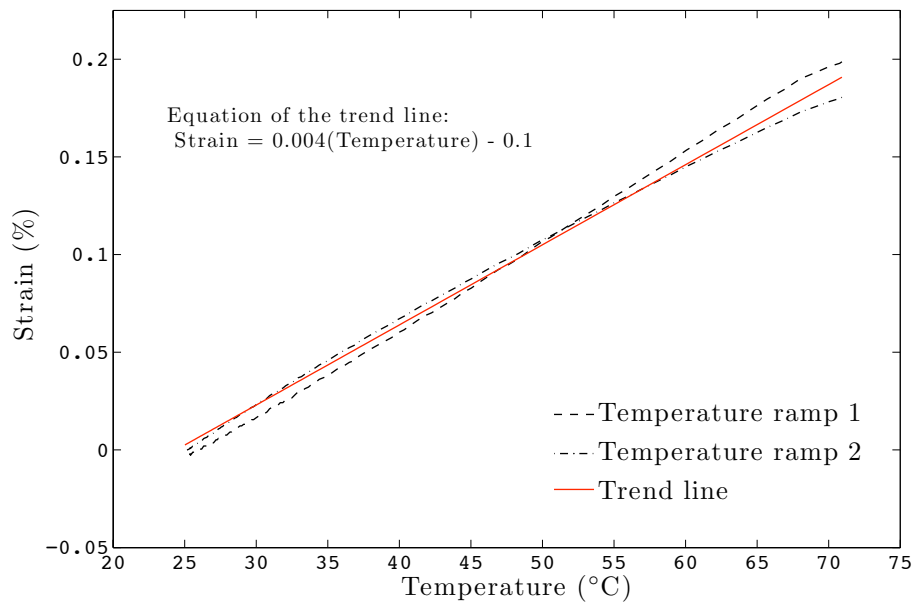
Figure 5.2 CTE of the epoxy resin

localizing the temperature where the storage modulus drop occurs.

Four prismatic specimens of 35 mm x 10mm x 3.65mm were submitted to a temperature ramp of 10°C/min. Tests were performed on a DMA Q800 machine and specimens were clamped in dual cantilever mode. T_g were determined from the intersection of the two storage modulus slopes. The parameters used for each test are presented in Table 5.1, together with the glass transition temperature found. Figure 5.3 presents one scan result of the epoxy system.

All test specimens were tensile loaded to 15 MPa during 60 seconds at least 24 hours before testing in order to eliminate specimens which could present defects. The specimens were loaded at room temperature and the stress level set in order to allow a full recovery of the material. Following these preliminary tests, a few specimens did break and were therefore not tested.

Creep-recovery tests and transient stress and temperature tests were repeated at least twice and a mean curve was used for the analyses. Figure 5.4 shows a typical deviation between experimental curves. Standard deviation on creep-recovery curves are presented in Table 5.2.

Table 5.1 Glass transition temperature of the epoxy resin obtained with DMA tests

Test	Frequency (Hz)	Amplitude	Force (N)	T_g
1	1	0.1	3	154.3
2	1	0.1	1	156.7
3	1	0.5	1	155.1
4	1	0.5	2	155.4
			Average	155.4
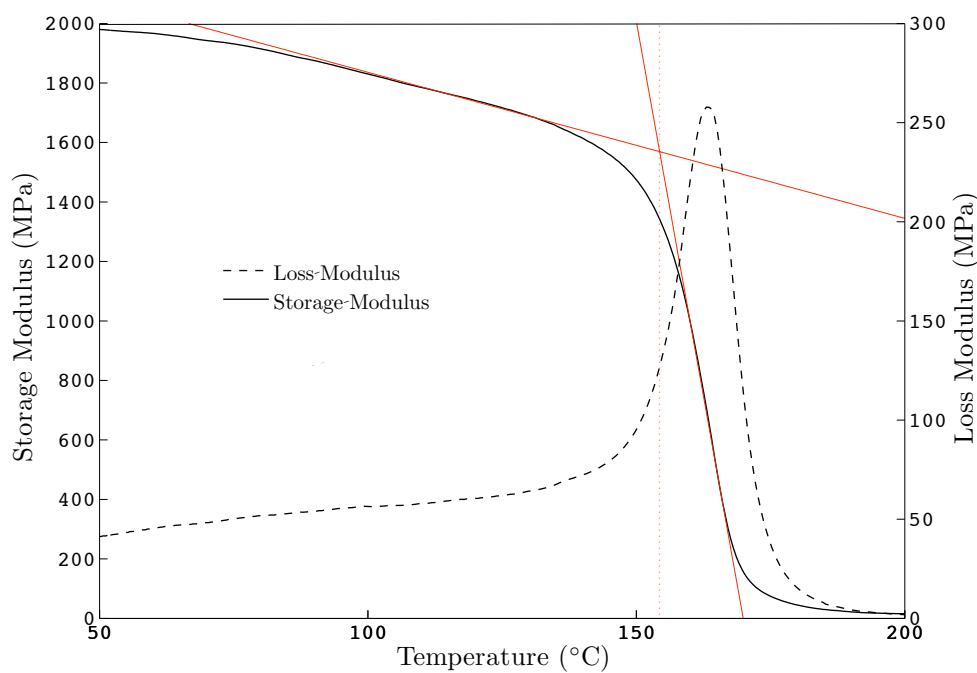
Figure 5.3 Based on DMA test results, the glass transition temperature of the cured thermoset resin was found to be around 155°C.
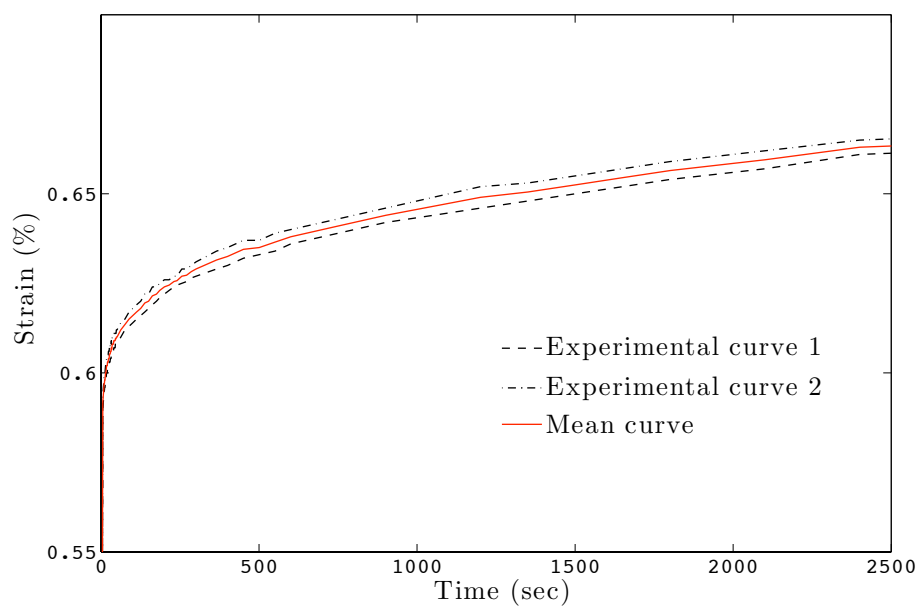
Figure 5.4 Typical deviation on experimental curves. The creep and recovery curves were obtained for 15MPa at 50°C and a mean curve was used for the analyses.

Table 5.2 Standard deviation on experimental curves

Stress (MPa)	5	10	15	5	10	15	5	10	transient
Temperature (˚C)	25	25	25	50	50	50	70	70	transient
Standard deviation ($\% \times 10^{-3}$)	12.1	94.0	101.9	76.2	80.4	87.9	87.5	79.8	65.9

5.4 Article presentation and coherence with research objectives

The results presented in this thesis are mainly regrouped in the peer reviewed paper presented in section 6. The paper covers in details the second sub-objective proposed in this work. The response to uniaxial isothermal creep and recovery tests was investigated at various temperatures and stress levels. The properties of the material was characterized using a Schapery-type constitutive model that was verified through complex experimental tests under transient temperatures and stress levels. Then, the study investigated the potential of using complex stress and temperature histories for improving the nonlinearly viscoelastic response of the model and the approach conventionally used for obtaining the material parameters. All the data presented in the paper relied on the setup and the methodology presented in chapters 4 and 5.

CHAPITRE 6

MODELING AND EXPERIMENTAL MATERIAL PARAMETERS IDENTIFICATION OF A NONLINEARLY VISCOELASTIC EPOXY RESIN SUBJECTED TO THERMO-MECHANICAL LOADING

6.1 Abstract

This paper presents a study on the thermo-mechanical behavior of an epoxy resin. The response of the material was investigated through both unixial isothermal creep-recovery tests as well as time-varying stress and temperature histories. The material mechanical response was predicted using a new Schapery-type constitutive model. The study firstly verified the accuracy of using material parameters obtained from isothermal creep and recovery curves to predict the response of the studied material subjected to a complex thermo-mechanical history. Then, data coming from both isothermal creep-recovery tests and transient stress and temperature load histories were used for obtaining the material parameters. It was found that adding more data did not improve significantly the predictions. A new approach for obtaining the parameters of the model using a limited amount of data coming only from time varying stress and temperature histories was developed and evaluted. The predictions of the model identified with this set of data were acceptable. These results are a motivation for future research aiming at designing optimized tests for obtaining reliable material parameters with a limited amount of experimental data.

6.2 Introduction

Under significant thermo-mechanical loading conditions, polymer materials may exhibit a nonlinearly viscoelastic behavior. Adequate constitutive theories for polymers have to take in account these nonlinear effects and use representative experimental data for obtaining ma-

terial properties.

The effect of temperature on the viscoelastic behavior of polymers has been widely studied by means of the time-temperature superposition principle (TTSP) (Luo (2007), Olasz et Gudmundson (2005), Zhao (2008), for example). Based on the free volume theory, TTSP uses the effective time concept to compare creep and compliance responses obtained at different temperatures. The concept implies that relaxation times, which increase with temperature, can be related to those at a reference temperature by a simple multiplicative shift factor. One main application of the concept consists of predicting long-term creep responses of polymers using data from short time tests (Ohashi *et al.* (2002), Olasz et Gudmundson (2005), Zhao (2008), Luo (2007), for example). Materials that can be fully characterized by means of the TTSP are categorized as thermorheologically simple materials (TSM) while materials that do not obey the TTSP are called thermorheologically complex materials (TCM).

TCM exhibit several time-temperature dependent mechanisms (Harper et Weitsman (1985)) and require more complex models such as Schapery's nonlinear model. In this model, the time-dependent properties such as material compliance are defined using linearly viscoelastic parameters and nonlinearizing functions. These functions are used to introduce nonlinearities induced by stress, temperature, moisture, aging, etc. Various authors studied the influence of the temperature on TCM using Schapery constitutive theories. Sawant et Muliana (2007) extended a recursive-iterative algorithm, previously developed by Haj-Ali et Muliana (2004), for predicting the nonlinear thermo-mechanical viscoelastic behavior of an orthotropic material using Schapery's constitutive theories. The algorithm was implemented in a FE package and verified using data from literature. The model was then used to predict the behavior of two composite materials and the thermo-mechanical response of FM-73 under complex stress and temperature histories. Sawant et Muliana (2008) used a similar algorithm for predicting transient thermo-mechanical conditions of two different polymers and multi-axial viscoelastic

responses of adhesively bonded joints at various temperatures. Recently, Shah *et al.* (2009) studied the behavior of TCM using composite cylinders under a time-varying temperature field.

Material parameters in these models are commonly obtained by isothermal creep and recovery tests (Lou et Schapery (1971), Zaoutsos *et al.* (1998), Papanicolaou *et al.* (1999),for example). Tests are usually performed at a fixed temperature and then repeated to completely cover the range of temperatures required. However, this experimental approach for obtaining the temperature and stress dependence parameters of the models might not truly represents the thermo-mechanical behavior of the material subjected to complex in-service loading and temperature histories.

Several studies investigated polymer responses under time varying uniaxial load histories at room temperature. For example, G'sell et Jonas (1981) studied the stress response of seven common thermoplastics subjected to various tests under true strain control at room temperature. Transient strain rates were used during experimentation, interrupted by relaxation periods. Peretz et Weitsman (1982) studied the nonlinearly viscoelastic behavior of FM-73 adhesive. Standard creep and recovery tests were used to get the material properties for the model. The accuracy of the model was then verified by two-step creep tests and loading-unloading experiments. Nordin et Varna (2005, 2006) compared the use of one-step and two-step loadings and unloadings for obtaining the parameters of a Schapery's nonlinear viscoelastic model. The studies showed that the usage of two-step loadings for predicting the behavior of vinyl ester and paper composites leads to more accurate results. Lévesque *et al.* (2008) introduced an experimental procedure which considered the whole mechanical response of a polymer. The approach did not rely on creep and recovery tests. Complex loading and unloading paths were designed for accurately identifying the isothermal nonlinearly viscoelastic behavior of a thermoplastic. Results demonstrated the importance of using various

loading histories to validate the accuracy of the models. Dreistadt *et al.* (2009) proposed a characterization procedure for polycarbonate using repeated loading-unloading tests at different strain and stress levels, interrupted by periods of creep.

Similar studies for elevated isothermal temperatures were also conducted. Ruggles-Wrenn et Balaconis (2008) investigated the influence of stress-rate on the behavior of BMI 5250-4 at 191°C. The effect of the loading rate was studied with loading and unloading tests under various stress rates. The effect of prior loading history was explored through stepwise creep tests incorporating loading and unloading stress ramps with intermittent creep periods at several stress levels. Results showed that the creep response was significantly affected by the prior stress rate and prior loading history. The nonlinearly viscoelastic model used could hardly predict creep responses and loading-unloading behavior, especially for low loading rates. Falcone et Ruggles-Wrenn (2009) repeated the study on PMR-15 thermosetting polyimide at 288°C with similar conclusions. McClung et Ruggles-Wrenn (2008) characterized the effect of prior strain rate and prior strain rate history. Various complex strain histories incorporating intermittent relaxation periods at several strain levels were conducted at 288°C. They obtained the same conclusions as that of Ruggles-Wrenn et Balaconis (2008).

Rather than conducting isothermal testing for studying the influence of temperature, Peretz et Weitsman (1983) extended their work on nonlinearly viscoelastic behavior of FM-73 adhesive to incorporate the effect of temperature on the mechanical response. Creep and recovery experiments were carried out for several temperatures with the integration of a cool down to 30°C when removing the stress for the recovery period. Various levels of creep stresses under the influence of a constant temperature ramp were applied to validate the nonlinear model used. Ohashi *et al.* (2002) studied the response of polypropylene under transient temperatures. Compressive stress-strain curves were obtained under trapezoidal temperature waveforms. Harper et Weitsman (1985) summarized a methodology used to characterize the

time-temperature behavior of a thermorheologically complex material. The study concluded that the use of combined results from isothermal creep tests and complex transient temperature experimentations led to a greater correspondence between experimental results and model predictions.

The purpose of this paper is to evaluate the accuracy of using isothermal creep and recovery data to determine the nonlinear viscoelastic properties of an epoxy resin for predicting the general strain response under complex stress and temperature histories. This paper is organised as follows : Section 6.3 describes the experimental procedure ; Section 6.4 presents the tests carried out and the results obtained ; Section 6.5 uses the time-temperature superposition principle to demonstrate that the material used in this study presents a typical TCM behavior. Section 6.6 introduces the time-dependent model used for modeling the epoxy resin mechanical response and describes the methodology used to determine the material parameters. The viscoelastic response of the material is then verified under complex stress and temperature histories in Section 6.7. In Section 6.8, the results are compared to those of a model using both isothermal creep-recovery curves and transient stress and temperature data for obtaining the material parameters. Then, a new approach presented in Section 6.9 attempts to obtain the model parameters from complex loading and temperature histories for predicting creep-recovery curves. The originality of this paper lies in the model used for predicting the material mechanical response and in the fact that both temperature and stress varying histories were used for identifying and validating the model thus obtained.

6.3   Experimental procedure

6.3.1   Material and specimens

The material studied consisted of an EPON 862 resin mixed with an Epikure 3300 (amine) curing agent at 24.8phr. The epoxy system was molded in rectangular flat molds and followed a cure schedule of 10 hours at room temperature, 1.5 hours at 82°C and 1.5 hours at 150°C.

Tensile testing specimens were obtained by waterjet cutting. ASTM type I tensile specimens were used for all the specimens but extended straight ends were employed to allow an adequate gripping of the specimens outside the furnace (see Section 6.3.2).

6.3.2 Experimental Setup

The tensile tests were carried out with a servocontrolled MTS mechanical testing machine. The experimental setup showed in Figure 6.1 was composed of a MTS 653.04 high temperature furnace with three heated zones, independently controlled by a MTS 409.83 temperature controller. The MTS testing machine had a 25kN (5.5Klbs) load cell and MTS 647.01A hydraulic grips with water-cooled wedges. For creep and recovery tests, strains were measured using a MTS 632.42 high temperature extensometer that had a 0.5 inch gauge length. Vishay EA-06-125TM-350 strain gauges were preferred to the extensometer for constant displacement rate tensile tests to avoid damaging the device in case of specimen failure. The strain gauges were bonded using Vishay M-Bond 200 adhesive.

6.3.3 Temperature Control

Temperature control was achieved by controlling the air temperature surrounding the furnace heaters with the MTS controller while monitoring the specimen temperature with thermocouples. A specifically designed fixture for attaching the thermocouples was used in order to obtain a space-wise and time-wise constant temperature in the test section. This apparatus could be easily clipped on the specimen and measured the variation of the temperature at three different positions evenly distributed over a 1.5 inches length. The specimens were heated at approximately $2°C/min$ and were maintained at the target temperature for 25 min before the tests start. A $\pm\ 0.75°C$ uniformity was obtained along the specimen gauge length. This variation represents the maximum difference between temperatures read by the three thermocouples at any specific moment during a test. Moreover, each thermocouple reading remained within a range of $\pm\ 0.75°C$ during testing.
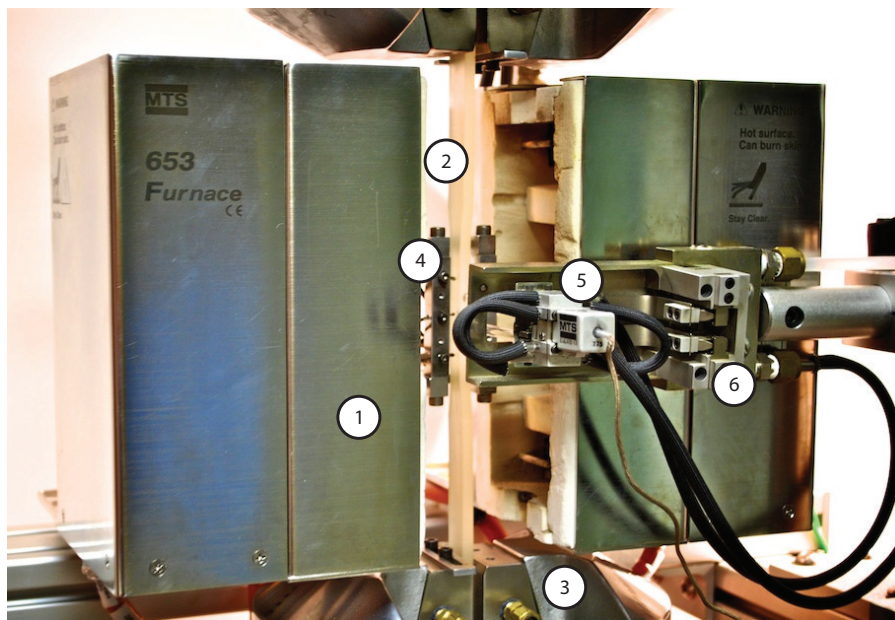
Figure 6.1 General view of the experimental setup. The two sides of the oven (1) are opened and an epoxy sample (2) is inserted into the grips (3). The thermocouples fixture (4) is attached to the specimen along with the extensometer (5). The extensometer is mounted to the specimen by two quartz rods. The extensometer support (6) has a spring that kept a low pressure on the extensometer in order to position the quartz rods on the specimen.

6.4 Tests and Results

6.4.1 Material properties verification

The coefficient of thermal expansion (CTE) and the glass transition temperature (Tg) of the material were determined prior to testing. The CTE of the material was measured with the high temperature extensometer for two specimens subjected to a temperature ramp of $1°C/min$. A CTE of $0.004\%C^{-1}$ was determined according to a mean slope obtained from both curves. It was found to be relatively constant for the tests performed. The Tg of the cured thermoset resin was determined using dynamic mechanical analysis (DMA). Four prismatic specimens of 35 mm x 10mm x 3.65mm were subjected to a temperature ramp of $10°C/min$. Tests were performed on a DMA Q800 machine and specimens were clamped in a dual cantilever mode. The Tg of the epoxy was found to be around $155°C \pm 1°C$.

6.4.2   Tensile tests at constant displacement rate

Tensile tests at the constant displacement rate of 5 mm/s were conducted on the epoxy resin at different constant temperatures, ranging from 25°C to 90°C. Two tests were performed at each temperature and the results showed minimal scatter. The purpose of these tests was to quantify the effect of the temperature on the general behavior of the epoxy resin for setting stress levels and temperatures to be used for creep tests. The average stress-strain curves obtained for each temperature are showed in Figure 6.2. The figure demonstrates that the behavior of the material is quite elastic at room temperature but becomes more compliant when the temperature is increased. Few tensile tests were conducted until failure. Preliminary tests revealed that at 90°C, the tensile strength of the resin dropped almost to half of that at 25°C.

6.4.3   Creep and recovery tests

Creep and recovery tests were performed at 25, 50 and 70°C. Creep stresses of 5, 10 and 15 MPa were tested for each temperature. The load history consisted of a two-hour creep phase followed by a eight-hour recovery. Temperatures, stress levels and creep-recovery times were set arbitrarily based on the results obtained from tensile tests. Creep loads as well as load removal were applied over a 5 seconds period. The tests showed that the material behaved nonlinearly at higher temperatures. Creep and recovery curves are presented in Figures 6.3 to 6.5, together with the predicted responses of the constitutive model described in section 6.6.

It should be noted that creep and recovery data for 15MPa at 70°C were not used during the material parameters identification, since a permanent plastic strain was obtained after the 8 hours recovery period and the model assumed a viscoelastic (i.e. non-plastic) behavior.
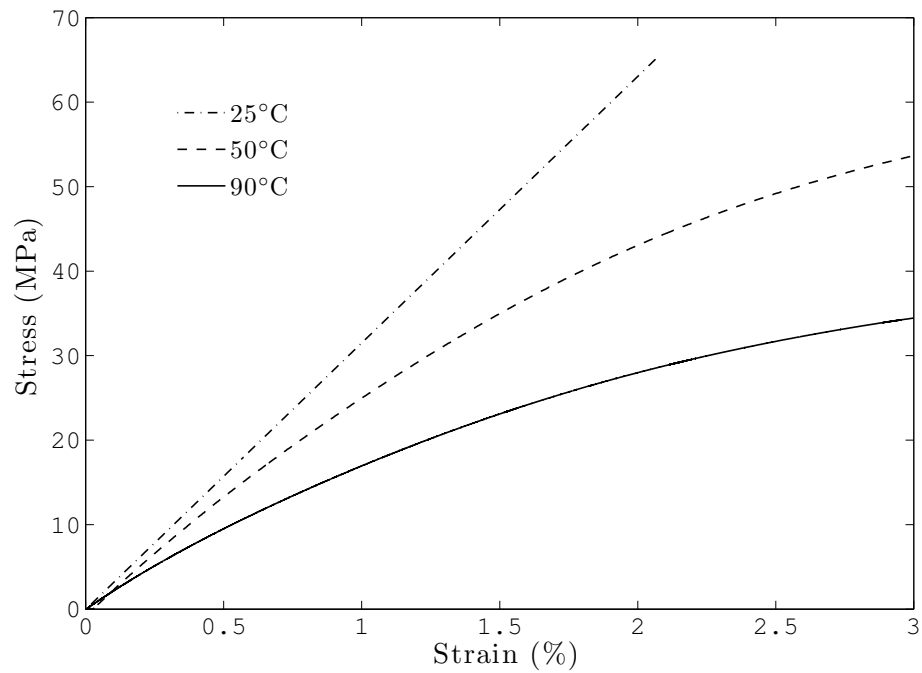
Figure 6.2 Isochronous stress strain curves for the epoxy resin for temperatures at 25°C, 50°C and 90°C at a constant displacement rate of 5mm/sec. For room temperature, the stress-strain relationship is quite linear and the material response is almost elastic while it becomes more compliant and viscoelastic for higher temperatures.
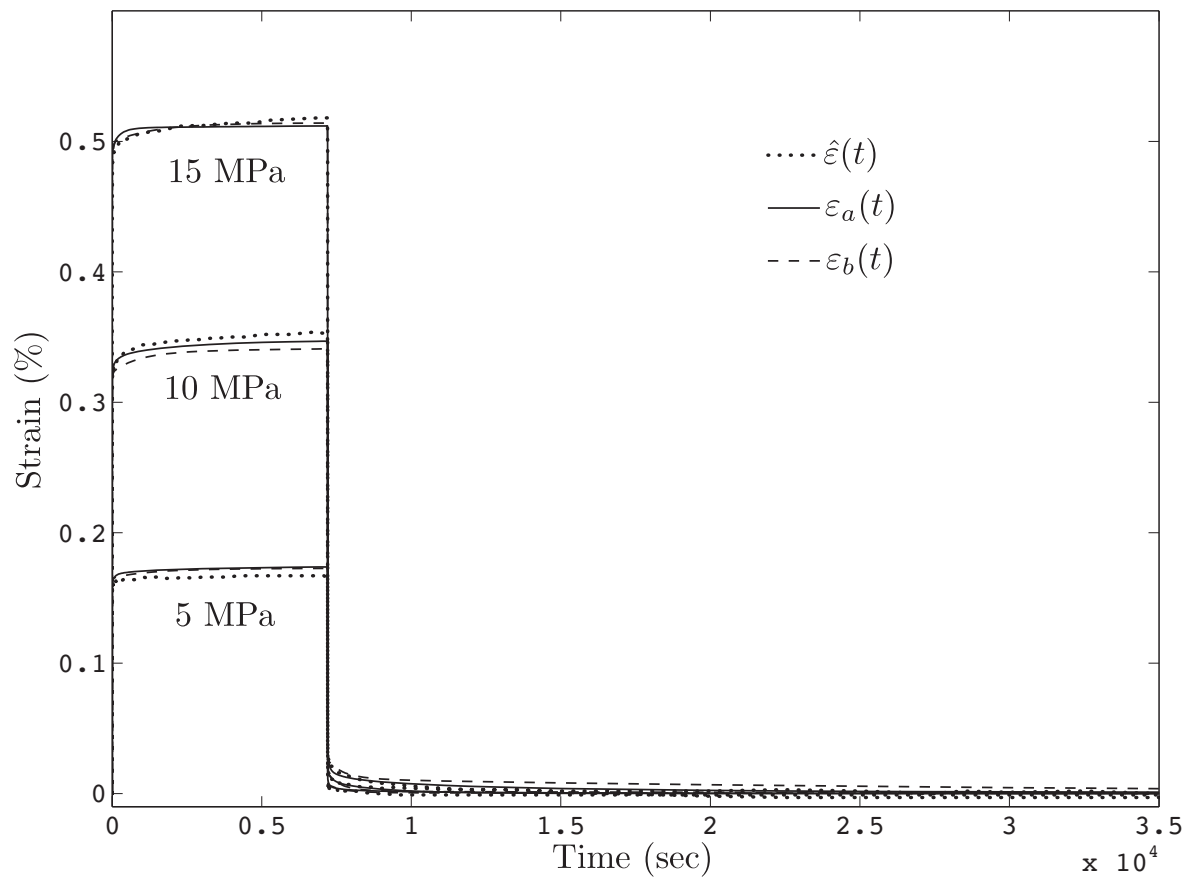
Figure 6.3 Creep and recovery curves at 25°C. Experimental data $\hat{\varepsilon}(t)$ and theoretical predictions of the constitutive law are showed for 5, 10 and 15MPa. $\varepsilon_a(t)$ shows predictions obtained for the first optimization approach using three variables λ_m while $\varepsilon_b(t)$ shows predictions of second optimization approach using ten constant λ_m.
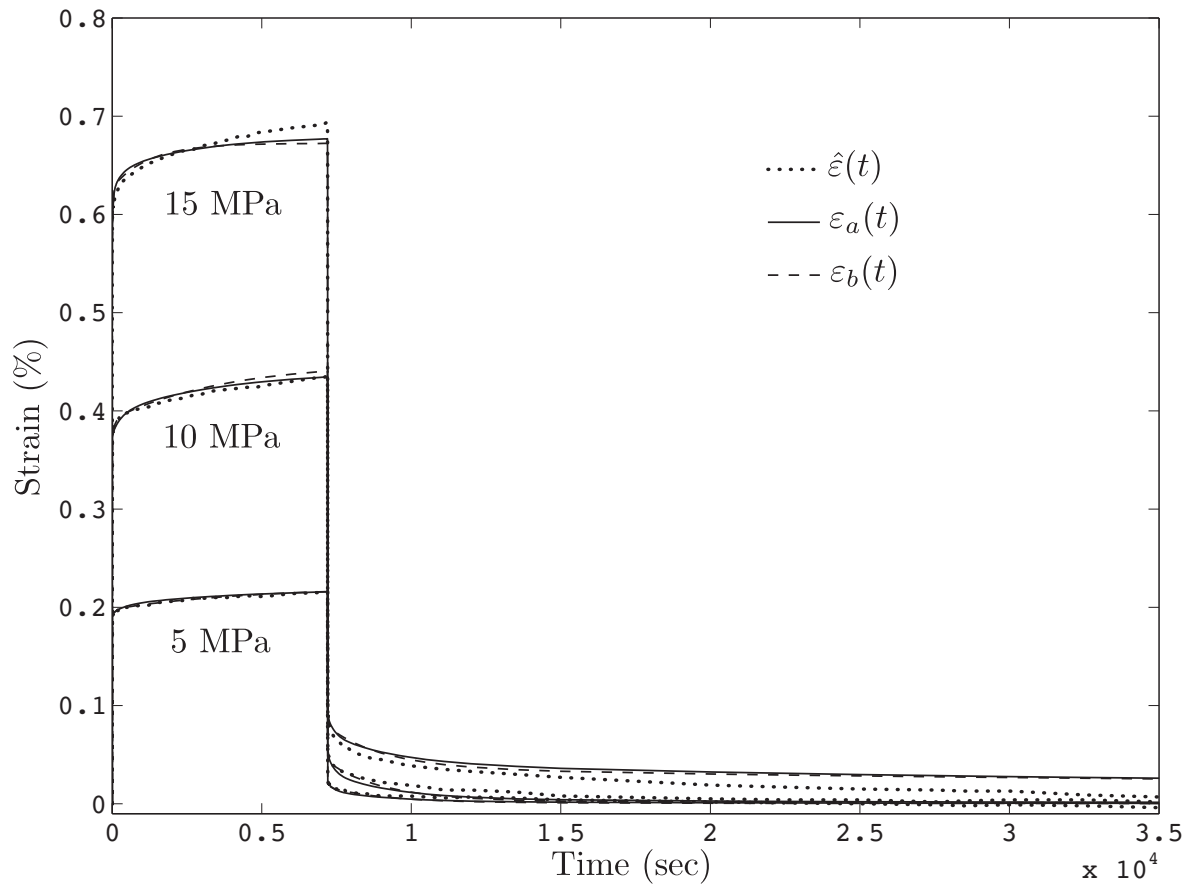
Figure 6.4 Creep and recovery curves at 50°C. Experimental data $\hat{\varepsilon}(t)$ and theoretical predictions of the constitutive law are showed for 5, 10 and 15MPa. $\varepsilon_a(t)$ shows predictions obtained for the first optimization approach using three variables λ_m while $\varepsilon_b(t)$ shows predictions of second optimization approach using ten constant λ_m.
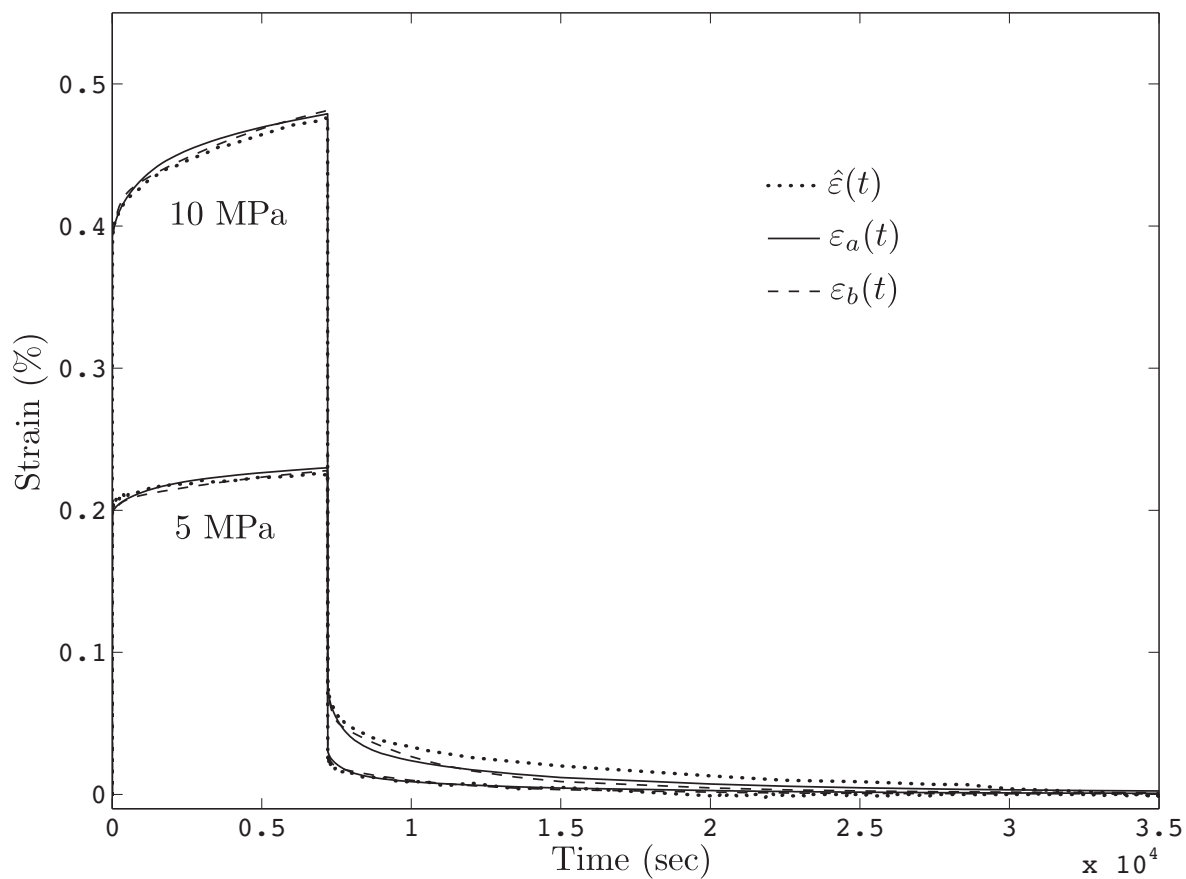
Figure 6.5 Creep and recovery curves at 70°C. Experimental data $\hat{\varepsilon}(t)$ and theoretical predictions of the constitutive law are showed for 5 and 10MPa. $\varepsilon_a(t)$ shows predictions obtained for the first optimization approach using three variables λ_m while $\varepsilon_b(t)$ shows predictions of second optimization approach using ten constant λ_m.

6.5 The Time-Temperature Superposition Principle

The time-temperature superposition principle uses the effective time concept to characterize the effect of the temperature on the response of viscoelastic materials. The effective time (θ) can be defined by noting that all relaxation that occurs over an infinitesimal period of time dt at temperature T is $\kappa(T)$ times of that occurring at a reference temperature T_R over a time period dθ (Brinson et Gates (2000)), so that

$$\theta(t) = \int_0^t \kappa(T(\zeta), \zeta) \mathrm{d}\zeta \tag{6.1}$$

where $\kappa(T)$ is called the temperature shift factor. Basically, the method consists in replacing the time variable in the material strain response by θ computed by means of Equation (6.1). By extrapolating the experimental data of various temperatures, the concept allows to set a single master curve which is representative of the material behavior for a specific stress state and temperature. If the temperature is kept constant over time, it can be seen that Equation (6.1) can be simplified as

$$\theta(t) = \kappa(T)t \tag{6.2}$$

This principle was applied to the creep part of the creep-recovery curves generated in this study, for each stress level. The creep curves were shifted in order to obtain, approximatively, a master creep curve for each stress level. Room temperature was set as the reference temperature. Since very few temperature levels were used in the study and tests were performed over a limited period of time, the shifted curves did not overlap in order to form an unambiguous master curve. This approach is nevertheless useful to assess if the material is thermorheologically simple or complex. The master curves obtained for each stress level are presented in Figure 6.6 on a logarithmic time scale. Creep curves at 50°C and 70°C were shifted horizontally by a singular factor of $\log \kappa_T$ presented in Table 6.1 in order to reproduce the behavior of the material at room temperature for each stress level. It can be seen that coefficients $\log \kappa_{T_{25-50}}$ and $\log \kappa_{T_{25-70}}$ change significantly according to the creep stress level.

Based on these observations, the material was assumed to be thermorheologically complex. A nonlinearly viscoelastic constitutive theory was therefore required in order to model the material behavior.

6.6 Nonlinearly viscoelastic model used in this study

6.6.1 Background

The model used in this study is a special case of the model that can be found in Schapery (1997). In thermodynamics of irreversible processes, the state of a material can be fully characterized by state functions of state variables. These state variables are divided into observable variables (the stresses in this case) and hidden variables (labelled as $\boldsymbol{\xi}$, for which no physical sense is given at this time). Combination of the first and second principles of thermodynamics leads to the differential equations (Schapery (1997)) :

$$a_1(\sigma, T)B_{rs}\dot{\xi}_s + a_2(\sigma, T)A_{rs}^{(3)}\xi_s + a_3(\sigma, T)A_{jr}^{(2)}\sigma_j(\sigma, T) + a_1\beta_r\Phi = 0 \qquad (6.3)$$

and to the constitutive equation :

$$\varepsilon_i(t) = -a_4(\sigma, T)A_{ij}^{(1)}\sigma_j - \left(\frac{\partial a_3(\sigma, T)}{\partial \sigma_i}A_{js}^{(2)}\sigma_j + a_3(\sigma, T)A_{is}^{(2)}\right)\xi_s = 0 \qquad (6.4)$$

where matrices $\mathbf{B}$ and $\mathbf{A} = \begin{bmatrix} \mathbf{A}^{(1)} & \mathbf{A}^{(2)} \\ \mathbf{A}^{(2)^T} & \mathbf{A}^{(3)} \end{bmatrix}$ are positive semi-definite and symmetric, $\boldsymbol{\beta}$ is a vector, $\Phi = T - T_R$ where T_R is the reference temperature, a_i are scalar functions of $\boldsymbol{\sigma}$ and T and $(\dot{\ })$ denotes time differentiation. Strains are obtained by solving Equation (6.3) for $\boldsymbol{\xi}(t)$

Table 6.1 Shifting factors $\log \kappa_T$ associated with the time-temperature superposition principle for each stress level

$\log \kappa_T$	5MPa	10MPa	15MPa
25° to 50°	1.5×10^{10}	1.5×10^4	1.0×10^8
25° to 70°	1.5×10^{12}	1.25×10^5	-
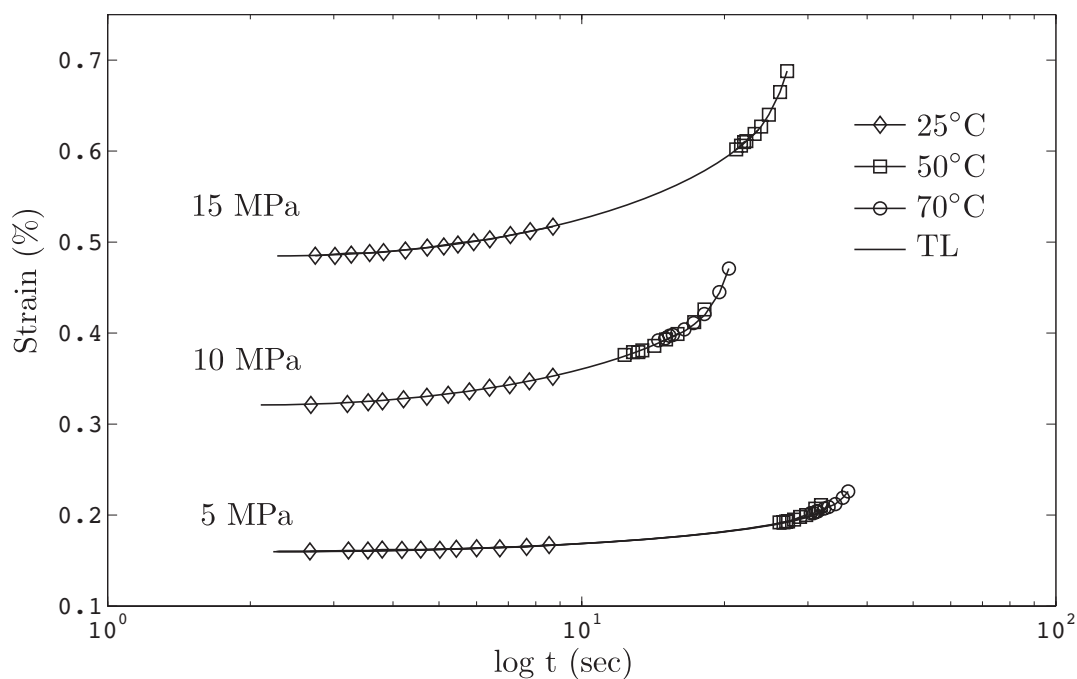
Figure 6.6 Master curves obtained using a trend line (TL) for 5, 10 and 15MPa set according to the TTSP a reference temperature of 25°C. Creep and recovery curves at 50°C and 70°C were shifted horizontally by a respective factor of $\log \kappa_T$ presented in Table 6.1.

and then replacing $\boldsymbol{\xi}$ in Equation (6.4). A reduced time is defined as

$$\Omega(t) = \int_0^t \frac{a_2(\chi)}{a_1(\chi)} \mathrm{d}\chi \tag{6.5}$$

and the strains can be expressed as

$$\begin{aligned}
\varepsilon_i(t) = \frac{\partial\varphi}{\partial\sigma_i} + \left(\frac{\partial a_3}{\partial\sigma_i}\sigma_j + a_3\delta_{ij}\right) \int_0^t \Delta S_{jk}\left(\Omega(t) - \Omega(\tau)\right) \frac{\mathrm{d}}{\mathrm{d}\tau}\left[\frac{a_3(\tau)}{a_2(\tau)}\sigma_k(\tau)\right]\mathrm{d}\tau \\
+ \int_0^t \Delta\alpha_i\left(\Omega(t) - \Omega(\tau)\right)\frac{\mathrm{d}\Phi(\tau)}{\mathrm{d}\tau}\mathrm{d}\tau
\end{aligned} \tag{6.6}$$

where δ_{ij} is Kronecker's delta and φ is a stress energy function associated with a nonlinearly elastic material. $\boldsymbol{\Delta}S$ and $\boldsymbol{\Delta}\alpha$ are respectively the transient compliance matrix and the thermal expansion vector which can be expressed as Prony series as

$$\Delta S_{ij}(t) = \sum_{m=1}^{M} S_{ij}^{(m)}\left(1 - \exp\left[-\lambda_m t\right]\right) \tag{6.7a}$$

$$\Delta\alpha_i(t) = \sum_{m=1}^{M} \alpha_i^{(m)}\left(1 - \exp\left[-\lambda_m t\right]\right) \tag{6.7b}$$

where $\mathbf{S^{(m)}}$ are positive semi-definite symmetric matrices and $\lambda_i \geq 0$ are the inverse of the retardation times. In this study, the material was assumed to be isotropic and only axial tests were performed on the specimens. Since the coefficient of thermal expansion was assumed to be constant and independent of the temperature (see section 6.4.1), $\Delta\alpha(t) = \alpha$. Therefore, the three-dimensional hereditary integral can be reduced to the stress-based uni-dimensional integral (Schapery (1969))

$$\varepsilon(t) = g_0 D^{(0)}\sigma(t) + g_1 \int_0^t \Delta S\left(\Omega - \Omega'\right)\frac{\mathrm{d}}{\mathrm{d}\tau}\left[g_2\sigma(\tau)\right]\mathrm{d}\tau + \alpha\Phi \tag{6.8}$$

where $\mathbf{D}^{(0)}$ is the elastic compliance matrix and the $g_j(\sigma, T)$ are

$$g_0(\sigma, T) = a_4; \quad g_1(\sigma, T) = \frac{\partial a_3}{\partial \sigma}\sigma + a_3; \quad g_2(\sigma, T) = \frac{a_3}{a_2}; \quad g_3(\sigma, T) = \frac{a_1}{a_2}. \tag{6.9}$$

6.6.2 Determination of the material parameters

Determination of the material parameters was done following an optimization process in which tests results were compared with the numerical solution of Equation (6.3). The numerical model used in this study was obtained in accordance with a strategy proposed by Crochon *et al.* (2010). The method consists of using the one-dimensional expression of equation (6.3) (obtained by removing the j subscripts) and replacing the a_i functions with the g_i functions of equation (6.9) to define an incremental model. Using a backward-Euler Finite Difference (FD) scheme, the incremental formulation can be written as :

$$\xi_r^{n+1} = \left(\delta_{rs} + \Delta t^n \frac{1}{g_3^{n+1}} A_{rs}^{(3)}\right)^{-1} \left[\delta_{sv}\xi_v^n - \Delta t^n \frac{g_2^n}{g_3^n} A_s^{(2)}\sigma^{n+1} - \Delta t^n \beta_s \Phi^{n+1}\right] \tag{6.10}$$

$$\varepsilon^{n+1} = -g_4^{n+1} A^{(1)}\sigma^{n+1} - g_1^{n+1} A_s^{(2)}\xi_s^{n+1} \tag{6.11}$$

where superscripts n and $n + 1$ refer to the quantity at the current time n and at the next time increment $n + 1$ and Δt is a time increment. Fitting the model to the experimental curves requires identifying a few material parameters such as the internal matrices $\mathbf{A}^{(1)}$, $\mathbf{A}^{(2)}$, $\mathbf{A}^{(3)}$and the nonlinearizing functions g_0, g_1, g_2 and g_3. For each time-step, the method requires consequently to firstly update the internal variable with Equation (6.10) and then the strain response using Equation (6.11).

The model was implemented into Matlab software and a least square method was used to optimize the various coefficients. The sum of squares, E, was defined as :

$$E = \sum_{k=1}^{M} \sum_{i=1}^{N(k)} \left(\hat{\varepsilon}^{(k)}(t_i) - \varepsilon^{(k)}(t_i)\right)^2 \tag{6.12}$$

where $\hat{\varepsilon}$ represents the experimental strain and ε is the predicted response of the model evaluated at all times t_i for which experimental data was recorded. Superscript k refers to the set of data points for a specific test and $N(k)$ is the corresponding number of data points for this set.

The nonlinearizing functions g_i were constrained to be positive and considered to be quadratic functions of both temperature and stress. The nonlinearizing functions were arbitrarily expressed as

$$g_i = (1 + \rho_i \sigma + \frac{1}{2}\eta_i \sigma^2)(1 + \gamma_i T + \frac{1}{2}\omega_i T^2) \tag{6.13}$$

A first estimate of the internal matrices was initially obtained using the creep-recovery curve obtained at room temperature and for a creep stress of 5 MPa, assuming $g_i = 1$. Stress-dependent parameters (ρ and η) and temperature-dependent parameters (γ and ω) were subsequently introduced into the model to optimize the nonlinearizing functions when considering data from creep and recovery curves at higher temperature and stress levels.

Two different approaches were attempted in order to find the best fitting of the material behavior. The first technique consisted of considering $\mathbf{A}^{(3)}$ as a diagonal matrix and optimizing all the parameters. When this is done, it can be showed that

$$A_{mm}^{(3)} = \lambda_m, \tag{6.14}$$

and the $S^{(m)}$ (now in 1D) of Equation (6.7a) are

$$S^{(m)} = \frac{1}{\lambda_m}(A_m^{(2)})^2, \tag{6.15}$$

and $D^{(0)}$ of Equation (6.8) is $D^{(0)} = -A^{(1)}$. For the first optimization approach, m was set

to $m = 3$. The following results were obtained :

$$A^{(1)} = -2.32 \times 10^{-2}; \quad \mathbf{A}^{(2)^T} = \begin{pmatrix} -5.48 \times 10^{-4} \\ 7.16 \times 10^{-5} \\ -1.77 \times 10^{-3} \end{pmatrix} \tag{6.16}$$

$$\mathbf{A}^{(3)} = \begin{pmatrix} 1.38 \times 10^{-2} & & \\ & 3.00 \times 10^{-4} & \\ & & 5.10 \times 10^{-1} \end{pmatrix} \tag{6.17}$$

The nonlinearizing functions are presented in Equations (6.18) where temperature is expressed in °C and stresses in MPa.

$$g_0 = (1 - 4.18 \times 10^{-3}\sigma - 7.34 \times 10^{-4}\sigma^2)$$
$$(1 + 1.90 \times 10^{-2}T - 2.66 \times 10^{-4}T^2) \tag{6.18a}$$

$$g_1 = (1 - 2.98 \times 10^{-3}\sigma - 2.29 \times 10^{-3}\sigma^2)$$
$$(1 + 9.84 \times 10^{-3}T - 2.35 \times 10^{-4}T^2) \tag{6.18b}$$

$$g_2 = (1 - 2.59\sigma - 2.89 \times 10^{-1}\sigma^2)$$
$$(1 + 3.27 \times 10^{-2}T - 1.01 \times 10^{-2}T^2) \tag{6.18c}$$

$$g_3 = (1 - 4.24 \times 10^{-1}\sigma - 6.51 \times 10^{-2}\sigma^2)$$
$$(1 - 1.02 \times 10^{-3}T + 2.04 \times 10^{-2}T^2) \tag{6.18d}$$

The second approach is similar to the first but the $A_{mm}^{(3)}$ were set a priori according to $A_{mm}^{(3)} = 10^{-(m-1)}$ for m ranging from 1 to 9, as presented in Equation (6.20). This is equivalent to fixing a retardation time per decade, as it is conventionally done when obtaining the parameters of a linearly viscoelastic constitutive theory. The results obtained for $A^{(1)}$ and

$\mathbf{A}^{(2)}$ are given in Equation (6.19).

$$A^{(1)} = -2.13 \times 10^{-2}; \quad \mathbf{A}^{(2)T} = \begin{pmatrix} 4.82 \times 10^{-5} \\ -1.70 \times 10^{-3} \\ -1.14 \times 10^{-3} \\ -4.85 \times 10^{-4} \\ 1.12 \times 10^{-4} \\ -4.48 \times 10^{-5} \\ -1.09 \times 10^{-7} \\ -2.68 \times 10^{-6} \\ 9.59 \times 10^{-7} \end{pmatrix} \tag{6.19}$$

$$\boldsymbol{A}^{(3)} = \begin{pmatrix} 1 & & & & & & & & \\ & 10^{-1} & & & & & & & \\ & & 10^{-2} & & & & & & \\ & & & 10^{-3} & & & & & \\ & & & & 10^{-4} & & & & \\ & & & & & 10^{-5} & & & \\ & & & & & & 10^{-6} & & \\ & & & & & & & 10^{-7} & \\ & & & & & & & & 10^{-8} \end{pmatrix} \tag{6.20}$$

The nonlinearizing functions obtained are presented in Equations (6.21), where temperature is showed in °C and stresses in MPa.

$$g_0 = (1 + 2.99 \times 10^{-3}\sigma + 2.29 \times 10^{-3}\sigma^2)$$
$$(1 + 9.84 \times 10^{-3}T - 2.35 \times 10^{-4}T^2) \tag{6.21a}$$

$$g_1 = (1 + 2.59\sigma - 2.89 \times 10^{-4}\sigma^1)$$

$$(1 + 3.27 \times 10^{-2}T - 1.01 \times 10^{-2}T^2)$$

$$\text{(6.21b)}$$

$$g_2 = (1 + 4.24 \times 10^{-1}\sigma - 6.51 \times 10^{-2}\sigma^2)$$

$$(1 - 1.02 \times 10^{-2}T + 2.04 \times 10^{-2}T^2)$$

$$\text{(6.21c)}$$

$$g_3 = (1 - 4.18 \times 10^{-3}\sigma - 7.34 \times 10^{-4}\sigma^2)$$

$$(1 + 1.90 \times 10^{-2}T - 2.66 \times 10^{-4}T^2)$$

$$\text{(6.21d)}$$

Experimental results show that the material becomes more compliant as stress increases (for a fixed temperature) or as temperature increases (for a fixed stress). Figure 6.7 plots the $g_i(\sigma, 0)$ and Figure 6.8 the $g_i(0, T)$ for the second approach, for illustration purposes. It can be seen that some g_i are not monotonous functions of their arguments. Even if the only thermodynamic requirement is that $g_i(\sigma, T) > 0$, it might be physically reasonable to expect a monotonic behavior for the nonlinearizing functions on the whole domain considered. Investigation of this behavior and the possibility of using g_i that are constrained to be positive and monotonous is let for future studies.

Comparisons between experimental and theoretical creep and recovery curves are showed in Figure 6.3 to Figure 6.5 for each temperature tested. On the figures, $\hat{\varepsilon}(t)$ refers to the experimental strain, $\varepsilon_a(t)$ to the predicted strain using the first approach and $\varepsilon_b(t)$ to the predicted strain using the second approach. Good agreement can be seen between experimental and theoretical curves for each temperature and stress level evaluated. The model fits very well the experimental data for both optimization approaches, although the second approach seems to deliver slightly more accurate results.
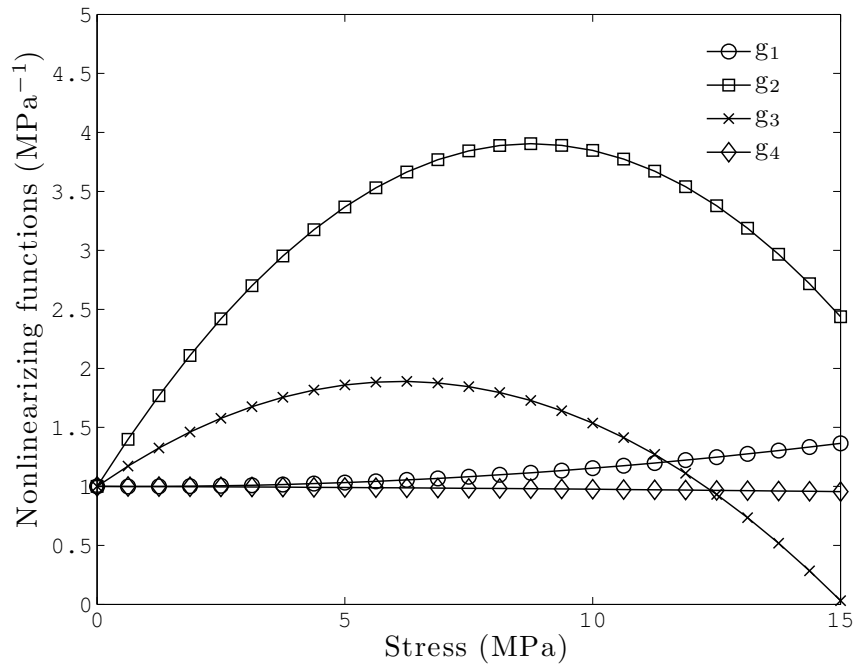
Figure 6.7 Stress dependence of nonlinearizing functions obtained by plotting $g_i(\sigma, 0)$ obtained from the second identification procedure.

6.7   Validation Tests

The model was evaluated by comparing predicted and experimental strains when the material was subjected to simultaneously varying stress and temperature histories. The loading path during the test included loading and unloading at different stress levels and stress rates, interrupted by periods of creep. The parameters obtained from the creep-recovery curves for the second optimization approach were used to predict the response to complex temperature and stress histories. Tests were conducted in load control mode. Figure 6.9 shows the stress and temperature histories used.

A comparison between experimental data and the predicted response of the model is showed in Figure 6.10. Very good agreement can be seen for the complete thermo-mechanical history. To appreciate the influence of nonlinearizing functions, the linear part of the model
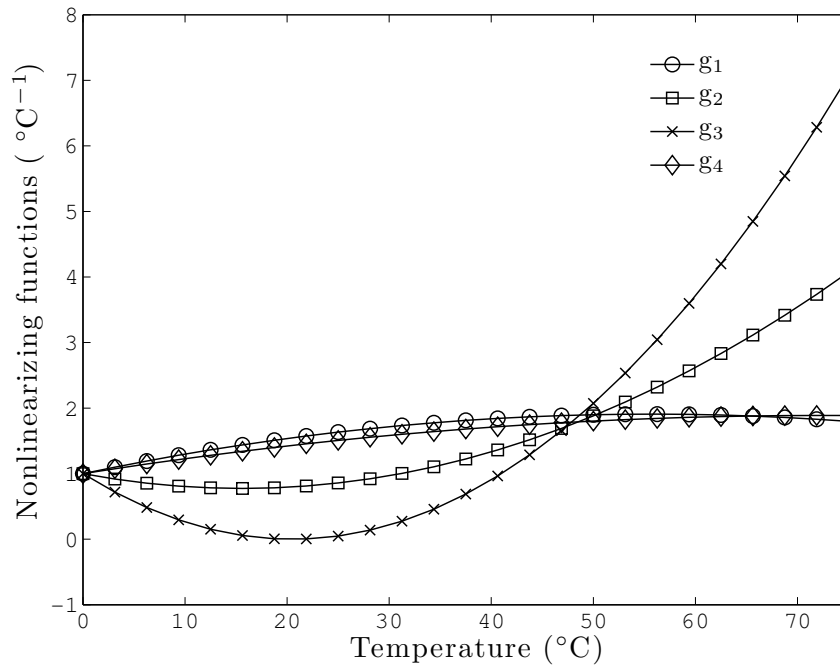
Figure 6.8 Temperature dependence of nonlinearizing functions obtained by plotting $g_i(0, T)$ obtained from the second identification procedure.
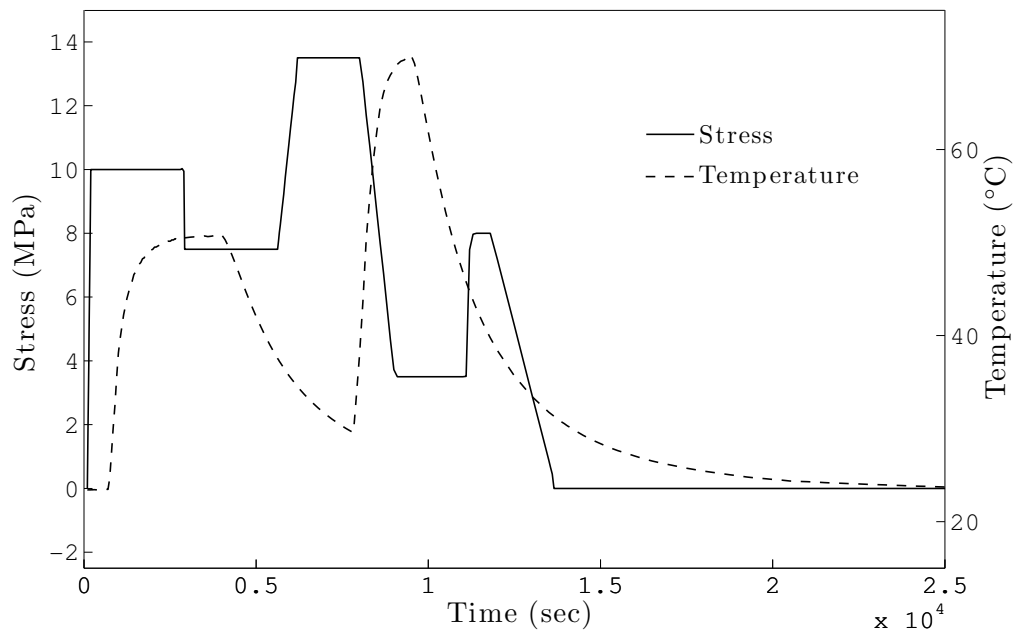
Figure 6.9 Stress and temperature history used for the validation of the identified behavior law. Five stress levels and two temperatures are reached during the test.

Figure 6.10 Validation of the identified behavior law under a transient loading and tempe-rature history. $\hat{\varepsilon}(t)$ refers to the experimental data, $\varepsilon_b(t)$ to the prediction of a nonlinearly viscoelastic constitutive theory and $\varepsilon_l(t)$ to the prediction of the linearly viscoelastic model

(i.e. model for which $g_i = 1$) was used to predict the strain response. The response predicted by the linear model is labeled as $\varepsilon_l(t)$ on the figure and it can be seen that it does not predict the strain response as well as the nonlinear model.
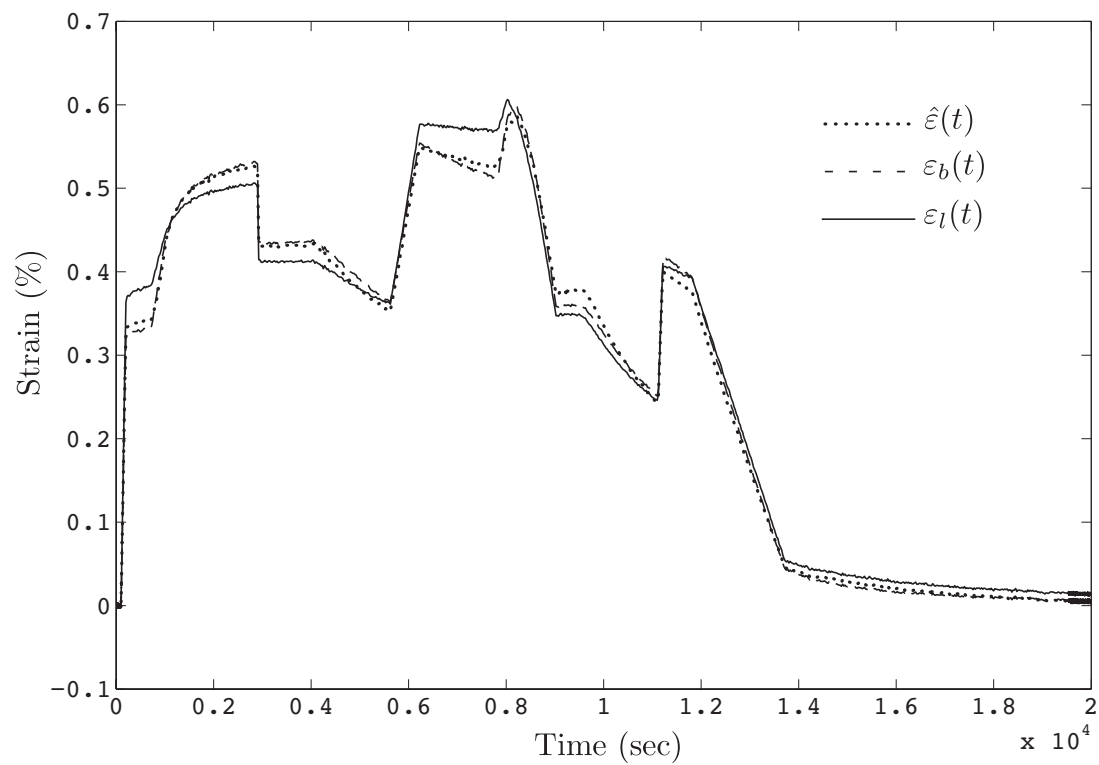
6.8 Obtaining the model parameter from all experimental data

All experimental data acquired during the creep-recovery tests and the complex stress and temperature history tests were then combined to find the model parameters. The purpose of the approach was to verify if a combination of transient stress and temperature data along with isothermal creep-recovery data could lead to a better representation of the material thermo-mechanical behavior. The determination of the material parameters was done following the second optimization process. The coefficients obtained for internal matrices $A^{(1)}$ and $\mathbf{A}^{(2)}$ are presented in Equation (6.22), while $\mathbf{A}^{(3)}$ was defined according to Equation (6.20). The nonlinearizing functions obtained are presented in Equations (6.23), where temperature is showed in °C and stresses in MPa.

$$A^{(1)} = -2.13 \times 10^{-2}; \quad \mathbf{A}^{(2)^T} = \begin{pmatrix} 1.02 \times 10^{-4} \\ 2.01 \times 10^{-3} \\ 5.06 \times 10^{-4} \\ -3.75 \times 10^{-4} \\ 1.53 \times 10^{-4} \\ 9.96 \times 10^{-5} \\ -1.56 \times 10^{-7} \\ -5.69 \times 10^{-6} \\ 1.64 \times 10^{-6} \end{pmatrix} \tag{6.22}$$

$$g_0 = (1 - 8.63 \times 10^{-3}\sigma + 1.62 \times 10^{-3}\sigma^2)$$
$$(1 + 6.18 \times 10^{-2}T - 1.39 \times 10^{-3}T^2) \tag{6.23a}$$

$$g_1 = (12.84 \times 10^{-1}\sigma - 1.31 \times 10^{-2}\sigma^2)$$
$$(1 - 7.58 \times 10^{-2}T - 5.89 \times 10^{-3}T^2)$$

<div align="right">(6.23b)</div>

$$g_2 = (1 + 4.08 \times 10^{-1}\sigma - 3.36 \times 10^{-2}\sigma^2)$$
$$(1 - 2.18 \times 10^{-2}T + 2.02 \times 10^{-3}T^2)$$

<div align="right">(6.23c)</div>

$$g_3 = (1 + 1.49 \times 10^{-3}\sigma - 4.68 \times 10^{-5}\sigma^2)$$
$$(1 + 2.56 \times 10^{-2}T - 4.01 \times 10^{-4}T^2)$$

<div align="right">(6.23d)</div>

The predicted strain using the material parameters obtained with all data is referred as $\varepsilon_c(t)$. Figure 6.11 presents results of the curve fitting optimization for the complex loading and temperature history while Figures 6.12 to 6.14 present a comparison between the experimental curves and the predicted creep and recovery curves for each temperature and stress level.

Results show hardly any difference between the predictions $\varepsilon_a(t)$, $\varepsilon_b(t)$ and $\varepsilon_c(t)$ for the complex thermo-mechanical test response. However, some differences can be seen for creep-recovery curves. When obtaining the material parameters with all experimental data, the model considerably underpredicted the strain response for the 10 MPa creep test at room temperature but gave a better prediction of the recovery part for the 15 MPa creep test at 50°C. Otherwise, this approach seemed to globally slightly improve the creep strain prediction for the highest loading level at 50°C and 70°C.

6.9 Obtaining the model parameter from complex loading and temperature histories

As can be seen from this study, obtaining the material parameters from creep-recovery curves requires considerable effort. It would be of particular interest to estimate the potential of using complex stress and temperature histories for obtaining the material parameters. Since the complex load histories cover the entire range of service stresses and temperatures,

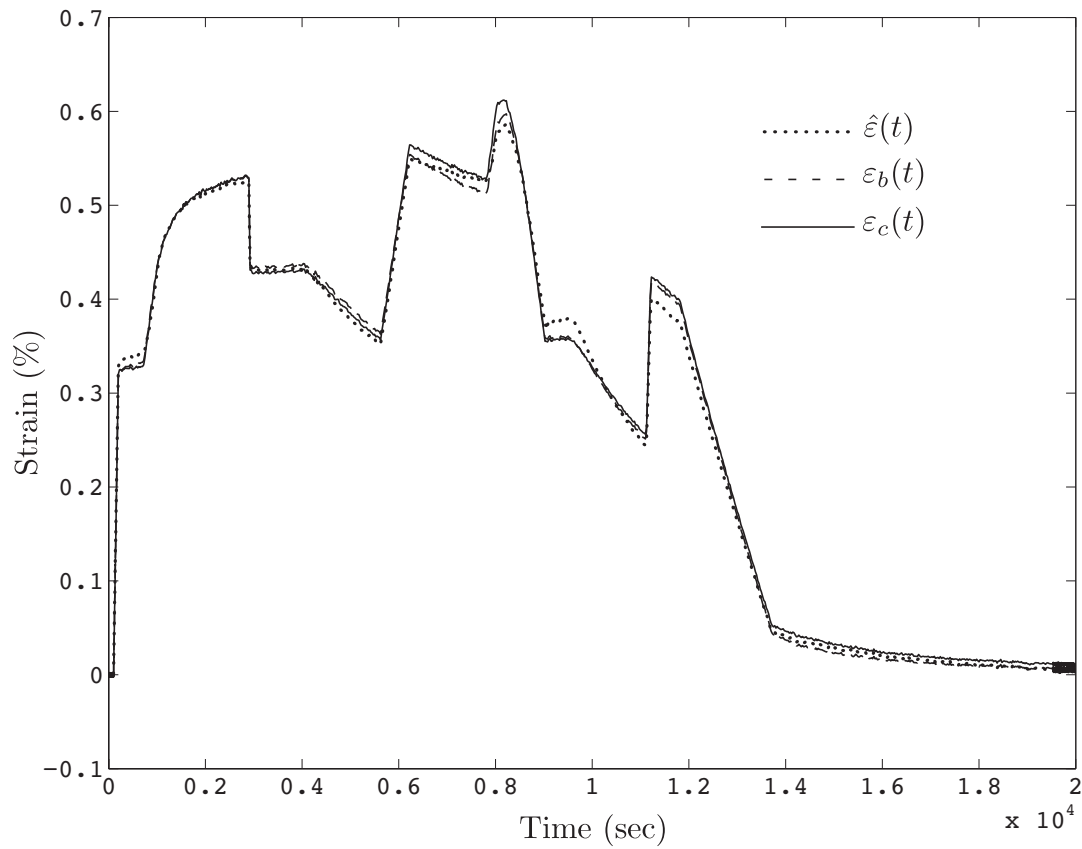Figure 6.11 Results of the curve fitting optimization with all experimental data for the complex thermo-mechanical history. $\hat{\varepsilon}(t)$ refers to the experimental data, $\varepsilon_b(t)$ to the predicted strain using the material parameters obtained with only the creep-recovery curves and $\varepsilon_c(t)$ to the predicted strain using the material parameters obtained with all data.

Figure 6.12 Results of the curve fitting optimization with all experimental data for creep and recovery curves at 25°C. Experimental data $\hat{\varepsilon}(t)$ and theoretical curves of the constitutive law are showed for 5, 10 and 15MPa. $\varepsilon_b(t)$ refers to the predicted strain using the material parameters obtained with only the creep-recovery curves and $\varepsilon_c(t)$ to the predicted strain using the material parameters obtained with all data.
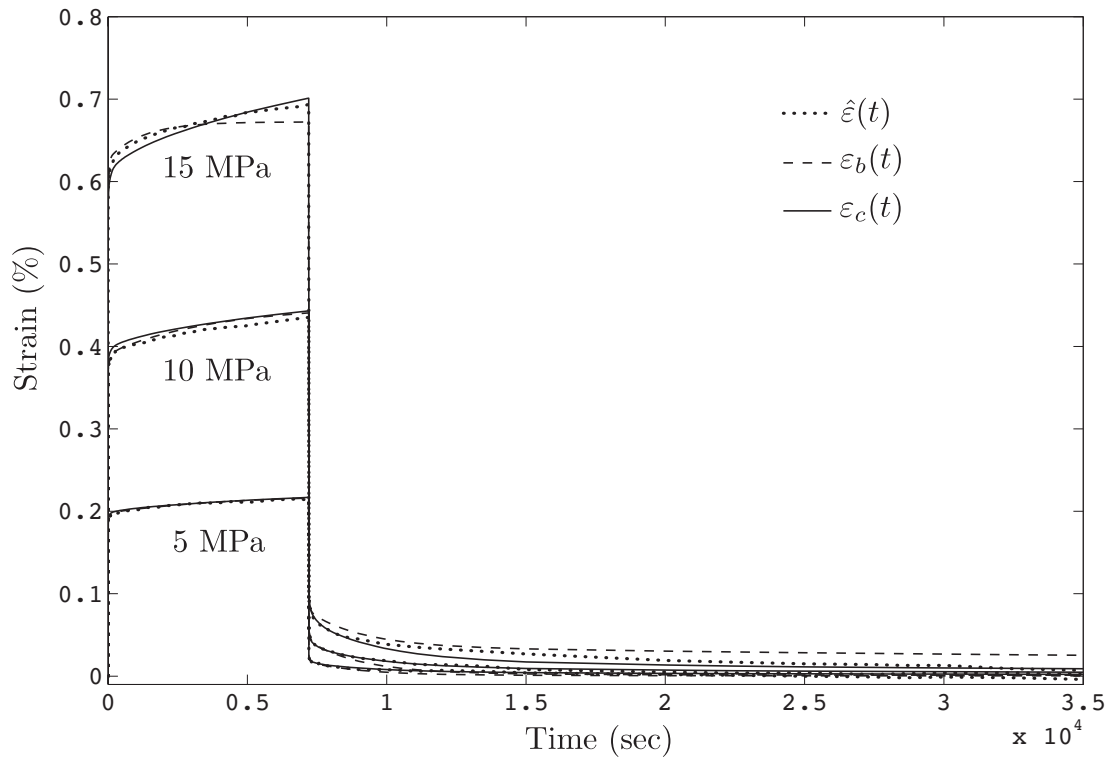
Figure 6.13 Results of the curve fitting optimization with all experimental data for creep and recovery curves at 50°C. Experimental data $\hat{\varepsilon}(t)$ and theoretical curves of the constitutive law are showed for 5, 10 and 15MPa. $\varepsilon_b(t)$ refers to the predicted strain using the material parameters obtained with only the creep-recovery curves and $\varepsilon_c(t)$ to the predicted strain using the material parameters obtained with all data.
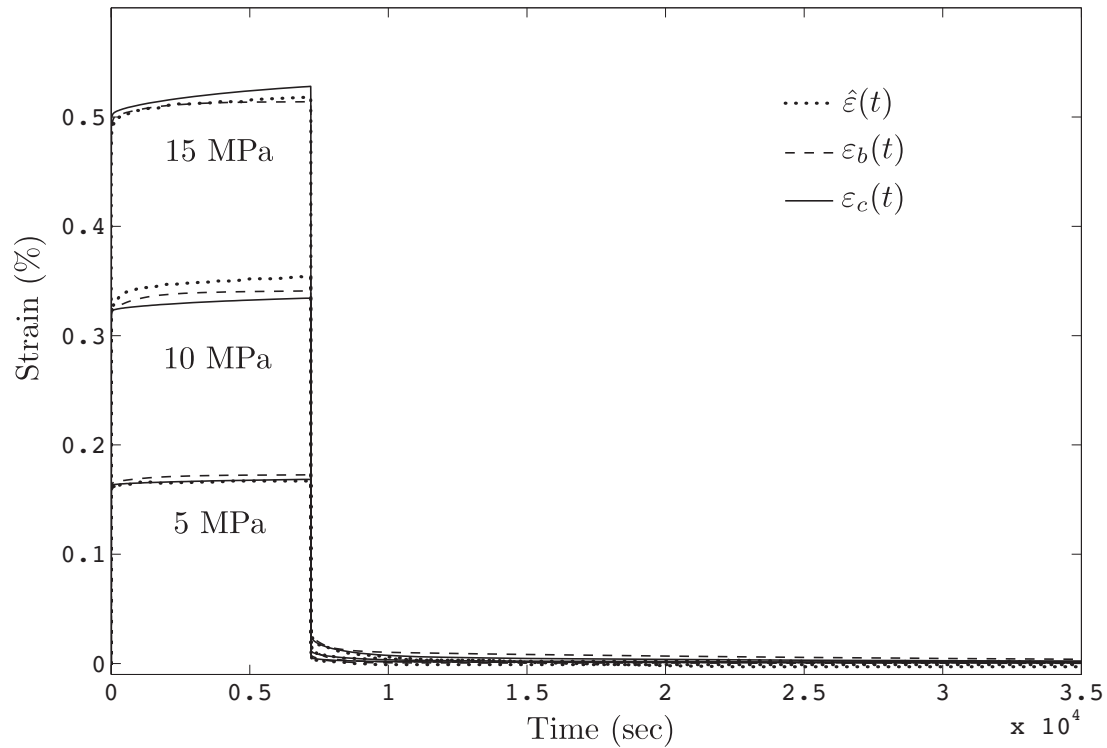
Figure 6.14 Results of the curve fitting optimization with all experimental data for creep and recovery curves at 70°C. Experimental data $\hat{\varepsilon}(t)$ and theoretical curves of the constitutive law are showed for 5, 10 and 15MPa. $\varepsilon_b(t)$ refers to the predicted strain using the material parameters obtained with only the creep-recovery curves and $\varepsilon_c(t)$ to the predicted strain using the material parameters obtained with all data.
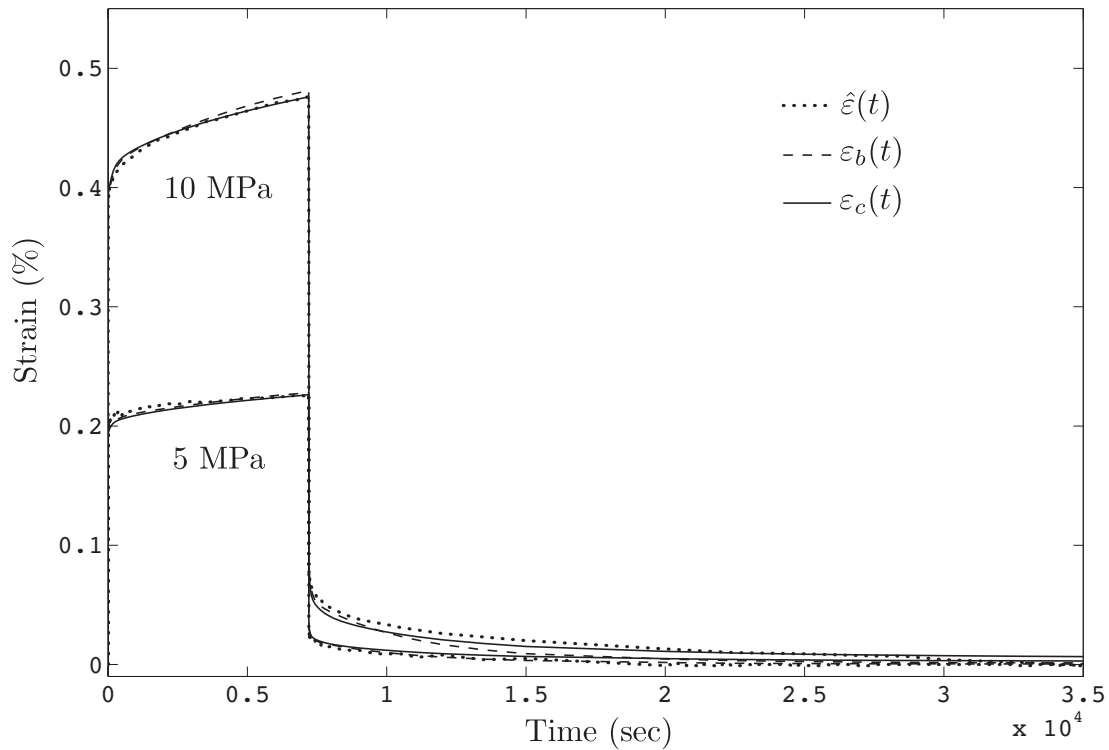
it is expected that fewer tests could provide the same information as many creep-recovery tests. This is the objective of this section.

Determination of the material parameters was done following the second optimization process of Section 6.6.2 using only the experimental data from the validation tests. The coefficients obtained for the internal matrices $A^{(1)}$ and $\mathbf{A}^{(2)}$ are presented in Equation (6.24), while $\mathbf{A}^{(3)}$ was defined according to Equation (6.20). The nonlinearizing functions obtained are presented in Equations (6.25), where temperature is showed in °C and stresses in MPa. The constitutive model thus obtained was then used to predict the creep and recovery curves for each temperature and stress level previously tested.

$$A^{(1)} = -2.34 \times 10^{-2}; \quad \mathbf{A}^{(2)^T} = \begin{pmatrix} 5.85 \times 10^{-5} \\ -1.52 \times 10^{-3} \\ -1.40 \times 10^{-3} \\ -3.38 \times 10^{-4} \\ 1.01 \times 10^{-4} \\ -4.55 \times 10^{-5} \\ -1.29 \times 10^{-7} \\ -2.01 \times 10^{-6} \\ 1.09 \times 10^{-6} \end{pmatrix} \tag{6.24}$$

$$g_0 = (1 - 1.22 \times 10^{-3}\sigma - 2.26 \times 10^{-4}\sigma^2)$$
$$(1 + 1.80 \times 10^{-2}T - 3.31 \times 10^{-4}T^2) \tag{6.25a}$$

$$g_1 = (1 - 2.38 \times 10^{-3}\sigma + 4.31 \times 10^{-3}\sigma^2)$$
$$(1 + 3.95 \times 10^{-2}T - 5.52 \times 10^{-4}T^2) \tag{6.25b}$$

$$g_2 = (1 + 8.71 \times 10^{-1}\sigma - 7.31 \times 10^{-2}\sigma^2)$$
$$(1 - 2.89 \times 10^{-2}T + 1.52 \times 10^{-3}T^2)$$

$$(6.25c)$$

$$g_3 = (1 + 2.81 \times 10^{-1}\sigma - 4.08 \times 10^{-2}\sigma^2)$$
$$(1 - 9.37 \times 10^{-2}T + 4.92 \times 10^{-3}T^2)$$

$$(6.25d)$$

The strains predicted by the model parameters obtained in this section are labeled $\varepsilon_d(t)$. Figure 6.15 presents results of the curve fitting optimization on complex loading and temperature histories while Figures 6.16 to 6.18 present a comparison between experimental curves and the predicted creep-recovery curves for each temperature and stress level. Obviously, since the optimization of the model parameters in this approach was performed only on the experimental data obtained during the validation test, the response of the model for the complex stress and temperature history was found very close to the experimental curve. However, a noticeable discrepancy can be seen between the experimental data and the predicted strains of the creep-recovery curves. The results are nevertheless encouraging, considering that single test was used for predicting relatively well the response of eight different tests.

6.10 Conclusion

Characterization of an epoxy resin was firstly done using a Schapery-type constitutive theory and data from isothermal creep and recovery tests at different temperatures and stress levels. The predictions of the model associated with the parameters obtained from these load cases, were compared against experimental data obtained from complex load histories (stress and temperature). Results have shown good agreement between the predictions and the experimental results. The very simple temperature and stress dependent nonlinearly viscoelastic model introduced in this study is potentially a good candidate for the mechanical behavior modeling of polymers subjected to thermo-mechanical loadings.
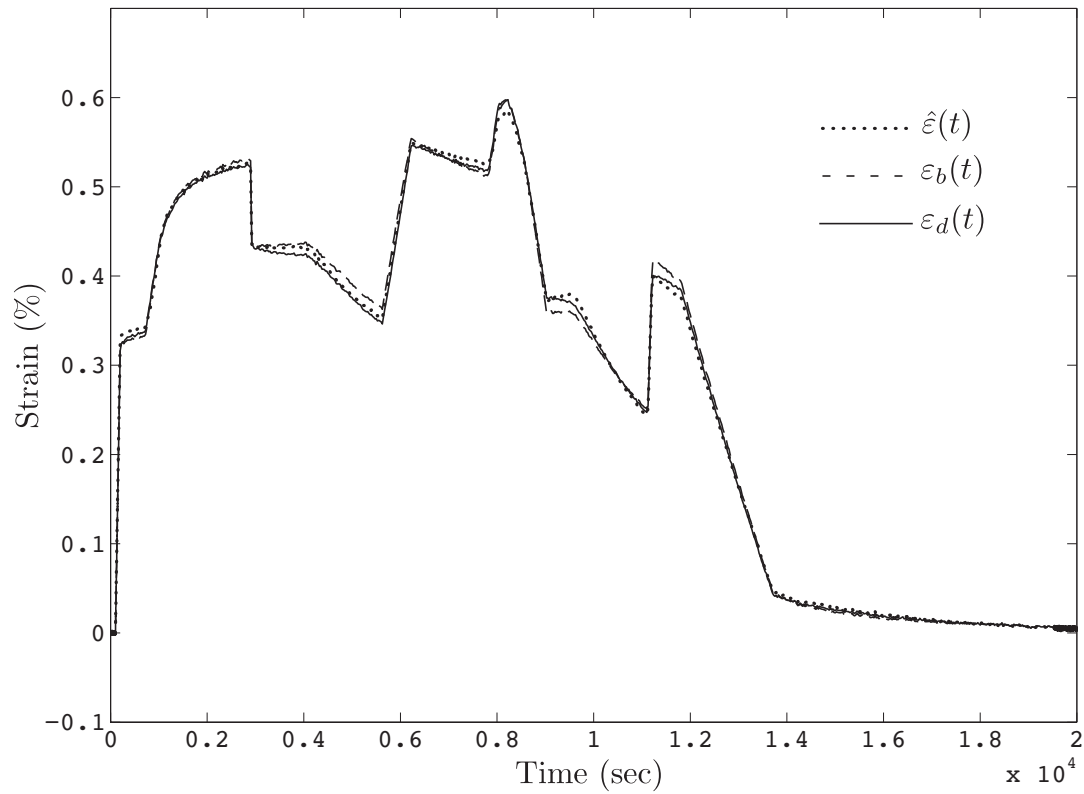
Figure 6.15 Results of the curve fitting optimization on complex loading and temperature histories. $\hat{\varepsilon}(t)$ refers to the experimental data, $\varepsilon_b(t)$ to the predicted strain using the material parameters obtained with only the creep-recovery curves, and $\varepsilon_d(t)$ to the model response using the material parameters obtained with complex loading and temperature histories.
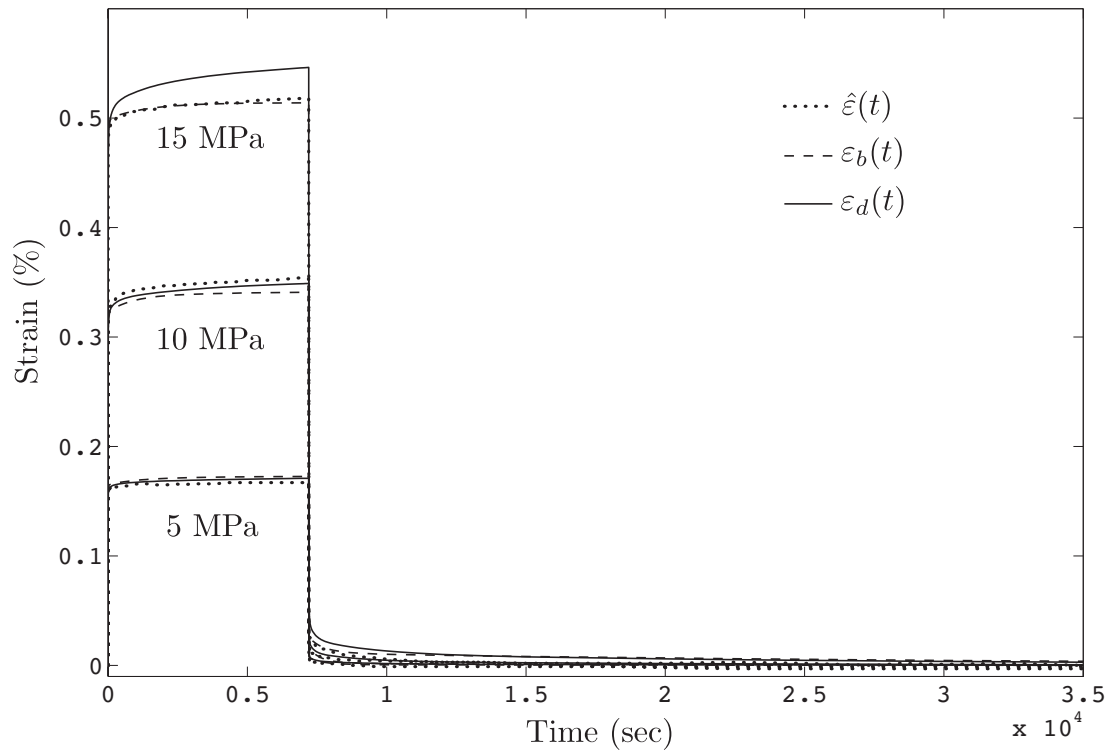
Figure 6.16 Validation of the constitutive model with creep and recovery curves at $25°$C. Experimental data $\hat{\varepsilon}(t)$ and theoretical predictions of the constitutive law are showed for 5, 10 and 15MPa. $\varepsilon_b(t)$ refers to the predicted strain using the material parameters obtained with the creep-recovery curves and $\varepsilon_d(t)$ to the model response using the material parameters obtained with complex loading and temperature histories.
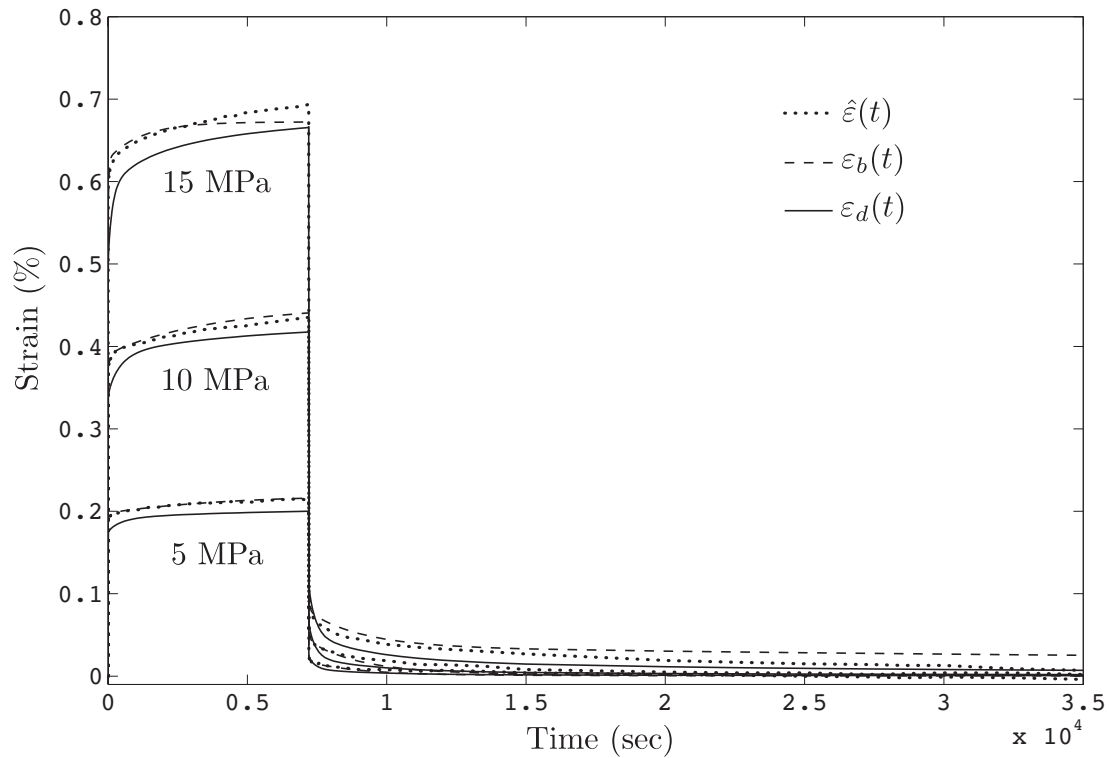
Figure 6.17 Validation of the constitutive model with creep and recovery curves at $50°$C. Experimental data $\hat{\varepsilon}(t)$ and theoretical predictions of the constitutive law are showed for 5, 10 and 15MPa. $\varepsilon_b(t)$ refers to the predicted strain using the material parameters obtained with the creep-recovery curves and $\varepsilon_d(t)$ to the model response using the material parameters obtained with complex loading and temperature histories.

Figure 6.18 Validation of the constitutive model with creep and recovery curves at $70°$C. Experimental data $\hat{\varepsilon}(t)$ and theoretical predictions of the constitutive law are showed for 5, 10 and 15MPa. $\varepsilon_b(t)$ refers to the predicted strain using the material parameters obtained with the creep-recovery curves and $\varepsilon_d(t)$ to the model response using the material parameters obtained with complex loading and temperature histories.
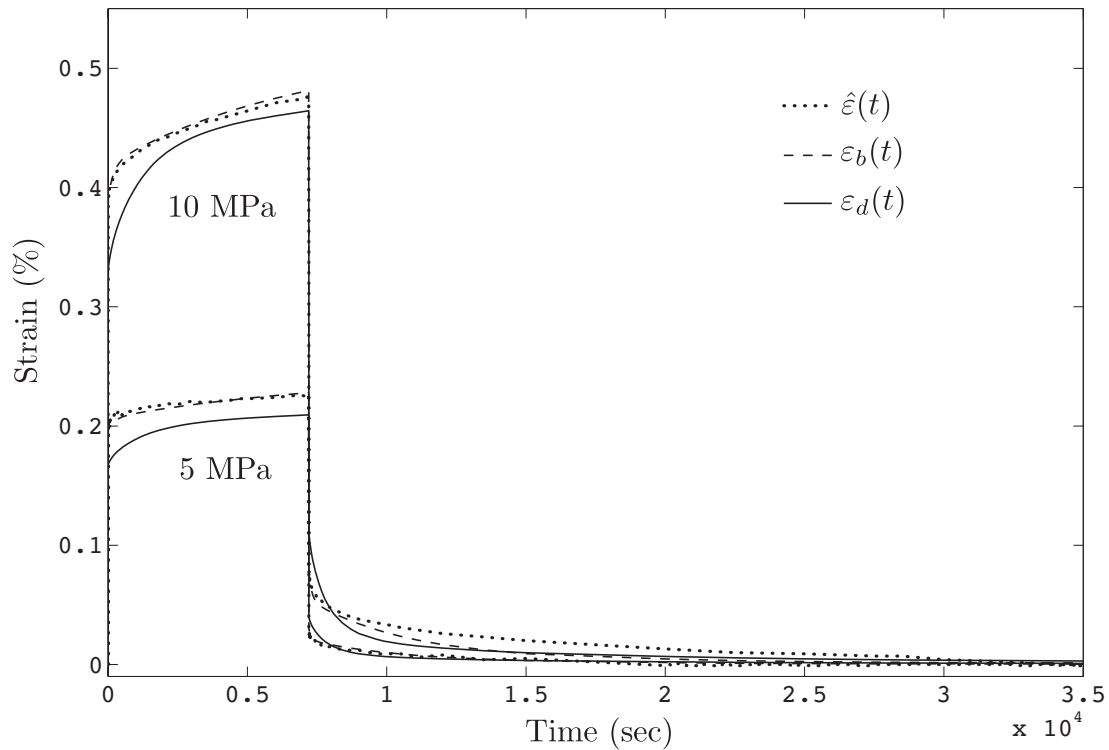
Both experimental data acquired during creep-recovery tests and complex stress and temperature history tests were then used to determine model parameters. The approach aimed at verifying that using data from transient stress and temperature tests in the optimization process could lead to a better representation of the material behavior. Globally, the strain responses were found to be pretty similar to that of the model using only isothermal creep and recovery curves. Based on these observations, it seems that the creep recovery data used for identifying the constitutive theory parameters was sufficient to deliver accurate predictions in the range of stresses and temperatures tested. This might suggest that there is an optimal amount of data to be used for obtaining material parameters above which not much information is gained.

A new approach for obtaining the material parameters was presented. The approach used data coming from complex stress and temperature histories to obtain the constitutive theory parameters and then predict the creep-recovery curves at different temperatures and stress levels. For this methodology, where only one test was conducted, results have shown a noticeable discrepancy between experimental and predicted curves. However, considering that the material parameters were obtained from a considerably smaller set of data, the results are promising. It is believed that designing optimized complex stress and temperature load histories might lead to a reduction of the experimental data required for obtaining material parameters. These optimized tests could be of considerable interest since material characterization is both time and resources consuming. The design of optimized tests is let for future studies.

In conclusion, the main contributions of this study are the introduction of a new nonlinearly viscoelastic model where both stress and temperature nonlinearities are taken into account and an example that complex stress and load histories have the potential of reducing the experimental effort for obtaining representative parameters for a nonlinearly viscoelastic

material.

CHAPITRE 7

GENERAL DISCUSSION

The objective of this chapter is to perform a critical evaluation of the work accomplished toward the completion of the two sub-objectives of the study, namely the development of the experimental setup for high temperature testing and the mechanical behavior modeling of the studied epoxy resin.

7.1 Evaluation of the experimental setup developed for high temperature testing

The experimental setup developed in the course of this study allowed for precise measurement of temperature, strain, displacement and force applied on the specimens, for a range of temperatures. It was successfully used for generating the experimental data required for obtaining the material parameters of the studied material. However, the setup could be improved.

The temperature on the specimens was manually controlled and modified at certain specific times during the complex thermo-mechanical tests to obtain the temperature history presented in Figure 6.9. This procedure required that the user stayed close to the setup through the whole duration of the tests. The automation of the temperature controller for programming complex temperature histories would therefore lead to a significant improvement of the experimental setup and might allow more flexibility in the temperature histories. Since the oven cannot be cooled artificially, its thermal properties will have to be carefully measured.

Moreover, measurements were performed and recorded for a constant frequency of 1Hz. This acquisition frequency was sufficient for obtaining rapid changes in the material behavior during stress and temperature ramps, but unnecessary information during creep and recovery periods was also stored. The method led consequently to large output files, which were difficult to manage. It would have been useful to be able to define a specific acquisition rate for each step of the thermo-mechanical history. Defining a real time adaptive sampling frequency based on the resulting strain rate, for example, could be of potential interest. This would require modifying the LabView code used for controlling the equipment.

7.2 Evaluation of the constitutive model and the methodology for determining the parameters of constitutive law

Parameters of the model were firstly obtained with data coming from isothermal creep and recovery tests at different temperatures and stress levels. The predictions of the model obtained were then compared with the experimental response to a complex thermo-mechanical history. Results have shown good agreement between the predictions and the experimental results and demonstrated that using isothermal creep and recovery data as well as the simple temperature and stress dependent nonlinearly viscoelastic model introduced in the study could lead to a good prediction of the general thermo-mechanical behavior of a polymer. However, obtaining the stress-dependent and temperature-dependent material parameters from creep-recovery curves requires considerable effort.

The study showed that adding transient stress and temperature histories to isothermal creep-recovery data for obtaining the model parameters did not lead to particular improvement of the model predictions. Since this last approach used more realistic experimental data for modeling the resin properties, it was expected to provide a better representation of the material thermo-mechanical response. These results therefore brought up the possibility that the model used in this study presented some limitations for characterizing the behavior of

the studied resin. Better constitutive theories, such as Schapery (1997), have been developed for modeling viscoelastic thermo-mechanical behavior of materials. These theories required however additional experimental data to properly define some of the material properties, such as the CTE. In this study, the CTE was simply assumed to be constant, which could have led to some discrepancy in the model responses. In the constitutive model, the form of the nonlinearizing functions was moreover arbitrarily constrained to quadratic functions of both stress level and temperature. Other less restrictive expressions might have been more representative. In addition, the nonlinearizing functions were not monotonous, which might be difficult to justify physically.

A considerable discrepancy was noticed when trying to predict creep and recovery curves with the model defined using data coming from complex stress and temperature loading histories. These results suggested the possibility that the complex stress and temperature history used did not bring enough information on the material behavior to properly define its viscoelastic properties. The complex thermo-mechanical history used in the study presented short creep periods and relatively fast stress and temperature ramps. The use of fewer complex stress and temperature history tests with longer periods and slower stress and temperature ramps could help getting more precise predictions. Despite the noticeable discrepancy between the predicted curves and the experimental data, the approach demonstrated a good potential for the characterization of polymers. The method could eventually allowing to precisely define the thermo-mechanical behavior of a viscoelastic material while bringing time and money saving to the industry by performing less experimental tests.

CHAPITRE 8

CONCLUSION AND RECOMMENDATIONS

8.1   Conclusion

The objectives of this project were to develop a reliable and precise experimental setup for conducting high temperature tensile testing on polymeric samples as well as to develop a data reduction procedure for obtaining the material parameters of a viscoelastic constitutive theory. Both objectives were reached. First, the experimental setup delivered accurate results and was relatively easy to use. Second, a new simple nonlinearly viscoelastic temperature and stress dependent model was introduced and its parameters were obtained through various procedures. This work led to a submitted journal publication to the journal *Mechanics of Time Dependent Materials*.

On the scientific aspect, the various procedures used for obtaining the material parameters suggest that there might be an optimal amount of data for obtaining reliable constitutive theories parameters. It has been exemplified that using a single set of data coming from complex temperature and stress loading histories can lead to acceptable model parameters. This study shown that there is a potential for defining optimal complex stress and temperature load histories for obtaining accurate material parameters with less experimental data than with the conventional approach relying on isothermal creep-recovery tests.

Although the project objectives were reached, some improvements could be made. First of all, the temperature control, even though very precise, was manual. It would be of considerable interest for the remaining of the collaborative project to automate it. In addition, the sampling frequency should be adjusted to collect the data that are of interest to the

study. On the modeling side, using physically based nonlinearizing functions might simplify the identification procedure as it is expected that less parameters will be used. In addition, forcing the nonlinearizing functions to be monotonous, for the material studied, might be more physically reasonable.

In conclusion, the main contributions of this study are :

1. The development and installation of an experimental setup for conducting high temperature tensile testing on polymeric samples. This setup will be used for the remaining of the collaborative project.

2. The introduction of a new and simple nonlinearly thermo-viscoelastic stress and temperature dependent model that could be used for modeling the mechanical behavior of other materials.

3. An example that there might exist an optimal amount of experimental data for obtaining material parameters and the potential for defining optimal complex stress and temperature loading histories tests for obtaining material parameters with reduced testing. This might be of considerable interest for the aerospace industry where testing is both time and economically consuming.

8.2   Recommendations

On the experimental side, future works should focus on automating the temperature control and sampling rate. A M.Sc.A. student is already working on these aspects.

On the modeling side, research should focus on using physically motivated nonlinearizing functions. The framework of Schapery's constitutive models is well adapted for the numerical implementation but lacks physical ground. The framework is quite flexible and it is expected that it might be possible to define with great success physically motivated nonlinearizing functions. This will require investigation of the microstructure and the microstructural de-

formation mechanisms.

Finally, it would be of interest to study theoretically techniques for designing optimal tests for obtaining reliable data in a reduced amount of testing. The approach could start with a constitutive theory with known parameters. Complex load histories could be simulated and the predicted response could be considered as experimental data. Then, algorithms would be developed for obtaining the material parameters. Different algorithms could be tested (classical, genetic algorithms, hybrid, etc.) in order to find the best experimental tests-algorithm combination.

REFERENCES

BRINSON, L. et GATES, T. (2000). *Viscoelasticity and Aging of Polymer Matrix Composites*, Pergamon Press, vol. 2. 333 – 368.

CROCHON, T., SCHÖNHERR, T., LI, C. et LÉVESQUE, M. (2010). On finite-element implementation strategies of schapery-type constitutive theories. Accepted for publication in *Mechanics of Time-Dependent Materials*.

DREISTADT, C., BONNET, A., CHEVRIER, P. et LIPINSKI, P. (2009). Experimental study of the polycarbonate behaviour during complex loadings and comparison with the boyce, parks and argon model predictions. *Materials and Design*, 30, 3126–3140.

FALCONE, C. et RUGGLES-WRENN, M. (2009). Rate dependence and short-term creep behavior of a thermoset polymer at elevated temperature. *Journal of Pressure Vessel Technology*, 131, 011403.

FINDLEY, W., LAI, J. et ONARAN, K. (1989). *Creep and relaxation of nonlinear viscoelastic materials : with an introduction to linear viscoelasticity*. Courier Dover Publications.

G'SELL, C. et JONAS, J. (1981). Yield and transient effects during the plastic deformation of solid polymers. *Journal of Materials Science*, 16, 1956–1974.

HAJ-ALI, R. et MULIANA, A. (2004). Numerical finite element formulation of the schapery non-linear viscoelastic material model. *International Journal for Numerical Methods in Engineering*, 59, 25–45.

HARPER, B. et WEITSMAN, Y. (1985). Characterization method for a class of thermorheologically complex materials. *Journal of Rheology*, 29, 49–66.

HOA, S. (2009). *Principals of the Manufacturing of Composite Material*. Destech Publications, Inc.

LÉVESQUE, M., DERRIEN, K., BAPTISTE, D. et GILCHRIST, M. D. (2008). On the development and parameter identification of schapery-type constitutive theories. *Mechanics of Time-Dependent Materials*, 12, 95 – 127.

LOU, Y. et SCHAPERY, R. (1971). Viscoelastic characterization of a nonlinear fiber-reinforced plastic. *Journal of Composite Materials*, 5, 208–234.

LUO, W. (2007). Application of time-temperature-stress superposition principle to nonlinear creep of poly(methyl methacrylate). *Key engineering materials*, 340, 1091–1096.

MARAIS, C. AND VILLOUTREIX, G. (1998). Analysis and modeling of the creep behavior of the thermostable PMR-15 polyimide. *Journal of Applied Polymer Science*, 69, 1983–1991.

MCCLUNG, A. et RUGGLES-WRENN, M. (2008). The rate (time)-dependent mechanical behavior of the pmr-15 thermoset polymer at elevated temperature. *Polymer Testing*, 27, 908–914.

MULIANA, A. et KHAN, K. (2007). A time-integration algorithm for thermo-rheologically complex polymers. *Computational Materials Science*, 41, 576–588.

MULIANA, A.H.AND SAWANT, S. (2009). Responses of viscoelastic polymer composites with temperature and time dependent constituents. *Acta Mech*, 204, 155–173.

NORDIN, L. et VARNA, J. (2005). Methodology for parameter identification in nonlinear viscoelastic material model. *Mechanics of Time-Dependent Materials*, 9, 57–78.

NORDIN, L. et VARNA, J. (2006). Nonlinear viscoplastic and nonlinear viscoelastic material model for paper fiber composites in compression. *Composites Part A : applied science and manufacturing*, 37, 344–355.

OHASHI, F., HIROE, T. et FUJIWARA, K. (2002). Strain-rate and temperature effects on the deformation of polypropylene and its simulation under monotonic compression and bending. *Polymer Engineering and Science*, 42, 1046–1055.

OLASZ, L. et GUDMUNDSON, P. (2005). Viscoelastic model of cross-linked polyethylene including effects of temperature and crystallinity. *Mechanics of Time-Dependent Materials*, <u>9</u>, 23–44.

PAPANICOLAOU, G., ZAOUTSOS, S. et CARDON, A. (1999). Further development of a data reduction method for the nonlinear viscoelastic characterization of frps. *Composites part A : Applied science and manufacturing*, <u>30</u>, 839–848.

PERETZ, D. et WEITSMAN, Y. (1982). Nonlinear viscoelastic characterization of fm-73 adhesive. *Journal of Rheology*, <u>26</u>, 245–261.

PERETZ, D. et WEITSMAN, Y. (1983). The nonlinear thermoviscoelastic characterizations of fm-73 adhesives. *Journal of Rheology*, <u>27</u>, 97–114.

RUGGLES-WRENN, M. et BALACONIS, J. (2008). Some aspects of the mechanical response of BMI 5250-4 neat resin at 191˚C : Experiment and modeling. *Journal of Applied Polymer Science*, <u>107</u>, 1378–1386.

SAWANT, S. et MULIANA, A. (2007). A thermo-mechanical viscoelastic analysis of orthotropic materials. *Composite Structures*, <u>83</u>, 61 – 72.

SAWANT, S. et MULIANA, A. (2008). A thermo-mechanical viscoelastic analysis of orthotropic materials. *Composite Structures*, <u>83</u>, 61–72.

SCHAPERY, R. (1969). On the characterization of nonlinear viscoelastic materials. *Polymer Engineering and Science*, <u>9</u>, 295 – 310.

SCHAPERY, R. (1997). Nonlinear viscoelastic and viscoplastic constitutive equations based on thermodynamics. *Mechanics of Time-Dependent Materials*, <u>1</u>, 209 – 240.

SHAH, S., MULIANA, A. et RAJAGOPAL, K. (2009). Coupled heat conduction and deformation in a viscoelastic composite cylinder. *Mechanics of Time-Dependent Materials*, <u>13</u>, 121–147.

VISHAY (2007). *Tech Note TN-504-1 : Strain Gage Thermal Output and Gage Factor Variation with Temperature.*

WILKES, C.E., SUMMERS, J., DANIELS, C. et BERARD, M. (2005). *PVC Handbook.* Hanser.

ZAOUTSOS, S., PAPANICOLAOU, G. et CARDON, A. (1998). On the non-linear viscoelastic behaviour of polymer-matrix composites. *Composites Science and Technology*, <u>58</u>, 883–889.

ZHAO, R. (2008). Application of time-ageing time and time-temperature-stress equivalence to nonlinear creep of polymeric materials. *Materials science forum*, <u>575</u>, 1151–1156.